Geol. Mag. **137** (5), 2000, pp. 495–516. *Printed in the United Kingdom* © 2000 Cambridge University Press

Coeval plutonism and metamorphism in a latest Oligocene metamorphic core complex in northwest Turkey

ARAL I. OKAY* & MUHARREM SATIR†

*İstanbul Teknik Üniversitesi, Avrasya Yerbilimleri Enstitüsü, Ayazağa 80626 İstanbul, Turkey
†Universität Tübingen, Institut für Mineralogie, Petrologie und Geochemie, Wilhelmstrasse 56, D-72074 Tübingen, Germany

(*Received* 18 November 1999; *accepted* 24 May 2000)

Abstract – A metamorphic core complex of latest Oligocene age crops out in the Kazdağ mountain range in northwest Turkey. The footwall of the core complex consists of gneiss, amphibolite and marble metamorphosed at 5 ± 1 kbar and 640° ± 50 °C. The average muscovite and biotite Rb/Sr ages from the gneisses are 19 Ma and 22 Ma, respectively, and imply high temperature metamorphism during latest Oligocene times. The hangingwall is made up of an unmetamorphosed Lower Tertiary oceanic accretionary melange with Upper Cretaceous eclogite lenses. The hangingwall and footwall are separated by an extensional ductile shear zone, two kilometres thick. Mylonites and underlying high-grade metamorphic rocks show a N-trending mineral lineation with the structural fabrics indicating down-dip, top-to-the-north shear sense. The shear zone, the accretionary melange and the high-grade metamorphic rocks are cut by an undeformed granitoid with a 21 Ma Rb/Sr biotite age, analytically indistinguishable from the Rb/Sr biotite ages in the surrounding footwall gneisses. The estimated pressure of the metamorphism, and that of the granitoid emplacement, indicate that the high-grade metamorphic rocks were rapidly exhumed at ~24 Ma from a depth of ~14 km to ~7 km by activity along the shear zone. The subsequent exhumation of the metamorphic rocks to the surface occurred during Pliocene–Quaternary times in a transpressive ridge between two overstepping fault segments of the North Anatolian Fault zone. The high-grade metamorphic rocks of the Kazdağ range are surrounded by voluminous calc-alkaline volcanic and plutonic rocks of Late Oligocene–Early Miocene age, which formed above the northward-dipping Hellenic subduction zone. The magmatic arc setting of the core complex and stratigraphic evidence for subdued topography in northwest Turkey prior to the onset of extension suggest that the latest Oligocene regional extension was primarily related to the roll-back of the subduction zone rather than to the gravitational collapse.

1. Introduction

The Aegean region is an area of present-day north–south extension above the Hellenic subduction zone (McKenzie, 1972; Le Pichon & Angelier, 1979). It is characterized by thin continental crust, high heat flow and widespread and diffuse seismicity (e.g. Berckhemer, 1977). Estimates for the beginning of extension in the Aegean region range from Late Oligocene (Lister, Banga & Feenstra, 1984; Buick, 1991; Seyitoğlu, Scott & Rundle, 1992) to Late Miocene (Le Pichon & Angelier, 1979; Dewey & Şengör, 1979). On the other hand, Eocene blueschists and eclogites in the Cyclades in the centre of the Aegean Sea (Schliestedt, Altherr & Matthews, 1987; Okrusch & Bröcker, 1990), and Eocene Barrovian type metamorphic rocks in the Menderes Massif (e.g. Şengör, Satır & Akkök, 1984) (Fig. 1) indicate that during the Middle Eocene the region was characterized by a thick continental crust (> 70 km). This is corroborated by widespread Eocene thrusts in the Menderes Massif and in the Taurides farther south (Gutnic *et al*. 1979; Collins & Robertson, 1998). There are two main theories for the origin of extension in the Aegean region. One is the gravitational collapse of the high topography created as a result of the Eocene crustal thickening (Berckhemer, 1977; Jolivet *et al.* 1994; Seyitoğlu & Scott, 1996). A second is the roll-back of the Hellenic subduction zone, creating a back-arc-type extension (Le Pichon & Angelier, 1981; Buick, 1991). In this study we provide structural, petrological and isotopic data from an extensional metamorphic core complex in northwest Turkey. The interpretation of the data indicates that the core complex formed during latest Oligocene times in the core of a coeval magmatic arc. The extension was top-to-the-north and was related to the roll-back of the Hellenic subduction zone.

* Author for correspondence: okay@itu.edu.tr

2. Geological setting

In northwest Turkey the deepest sections of the continental crust are exposed in the Kazdağ mountain range, which forms a structural and topographic dome of high-grade metamorphic rocks (Schuiling, 1959; Bingöl, 1969; Okay, Siyako & Bürkan, 1991; Pickett & Robertson, 1996; Okay *et al.* 1996) (Figs 2, 3). The Kazdağ range is elongated in a NE–SW direction and

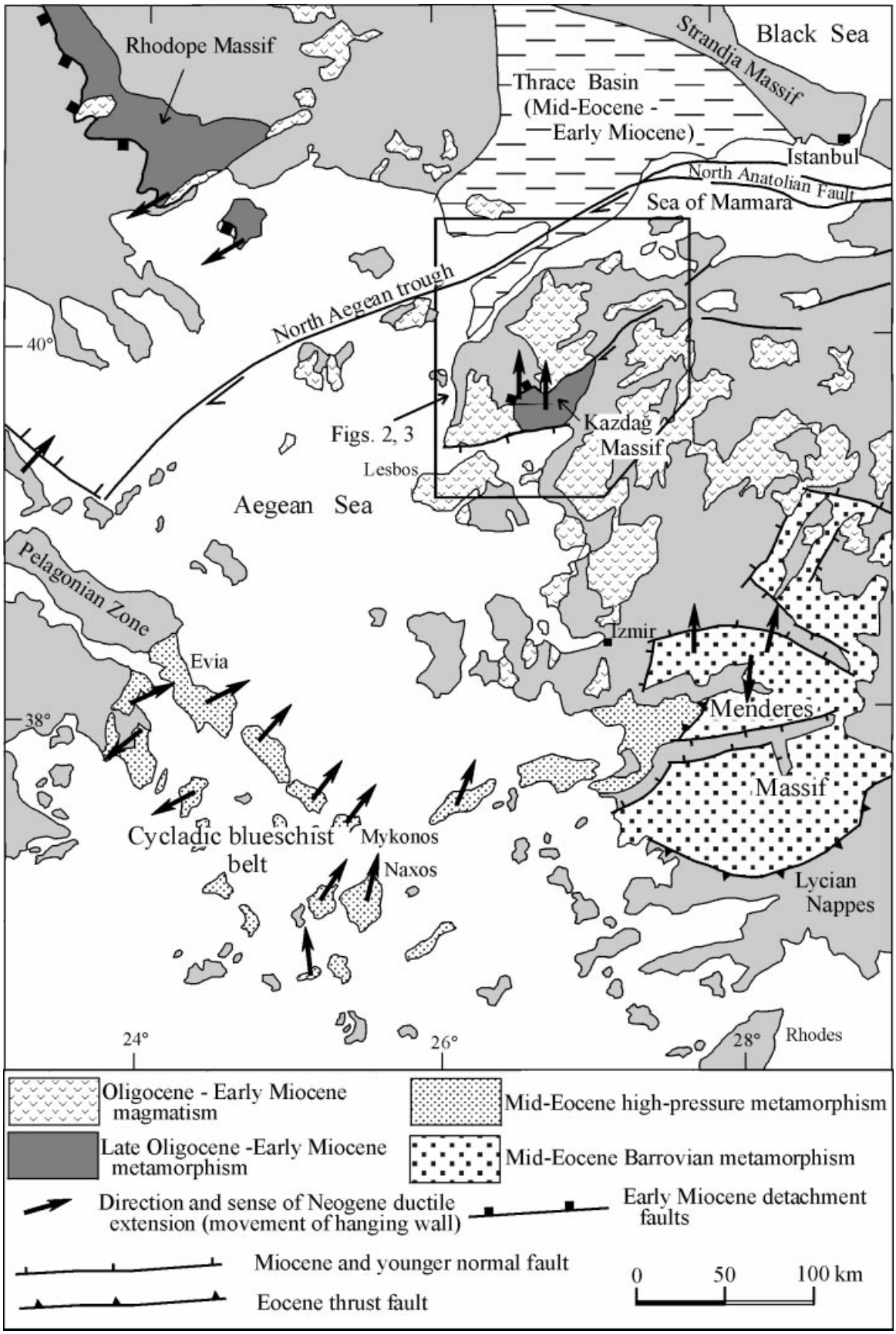

Figure 1. Tectonic map of the Aegean region showing the outcrops of Eocene and Late Oligocene–Miocene metamorphism and magmatism, and Neogene extension directions (data from Buick, 1991; Dinter & Royden, 1993; Gautier, Brun & Jolivet, 1993; Hetzel *et al.* 1995; Lee & Lister, 1992; Sokoutis *et al.* 1993; Wawrzenitz & Krohe, 1998; Walcott & White, 1998).

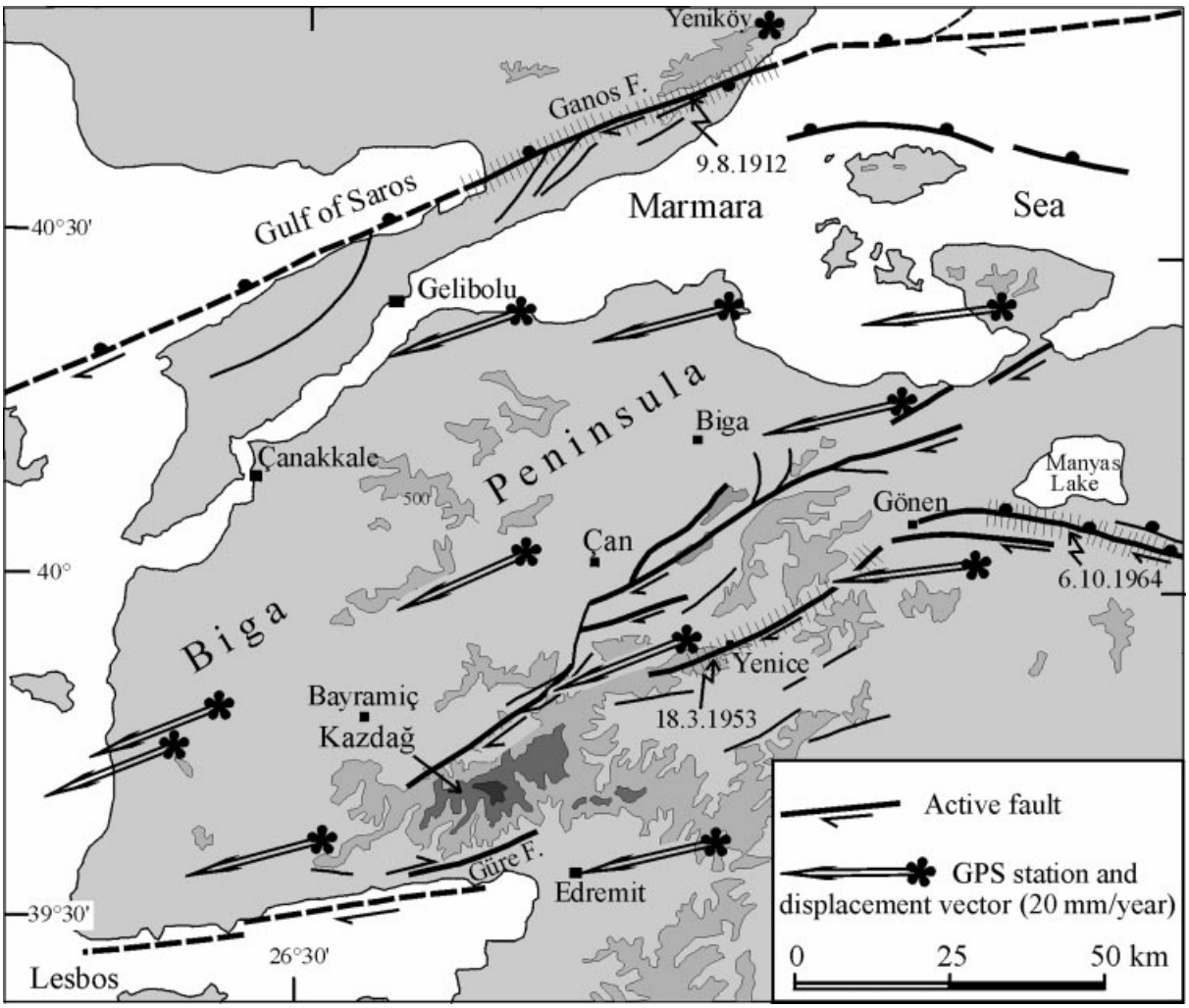

Figure 2. Topography and active faults in northwest Turkey. The contours are at 500, 1000 and 1500 metres. Fault segments ruptured during the earthquakes in this century are hachured. The stars and arrows indicate Global Positioning System (GPS) station localities and displacement vectors, respectively, with respect to a fixed station at Yenice north of the Ganos Fault (Straub & Kahle, 1995). Biga peninsula south of the Ganos fault is moving southwest at a rate of 2 cm/year. The Kazdağ range forms a transpressive ridge in a restraining step-over.

rises to 1767 metres above sea-level. It forms a topographic anomaly in the northeastern Aegean, where the average elevation is below 500 metres (Fig. 2). In the east the Kazdağ Massif is tectonically overlain by >5 km thick, strongly deformed Permo-Triassic basic volcanic and clastic rocks, whose lower parts show greenschist-facies regional metamorphism. These rocks, grouped under the Karakaya Complex, are in turn unconformably overlain by little-deformed Jurassic–Lower Cretaceous sandstones and limestones (Bingöl, Akyürek & Korkmazer, 1975; Okay, Siyako & Bürkan, 1991; Okay *et al.* 1996; Leven & Okay, 1996). In contrast, west of Kazdağ an oceanic accretionary melange, Late Cretaceous to Palaeocene in age, lies tectonically over the Kazdağ metamorphic rocks through an intervening shear zone (Fig. 3). The Kazdağ Massif, the shear zone and the accretionary melange are intruded by a latest Oligocene pluton (Fig. 4).

3. The Kazdağ Massif: footwall with latest Oligocene metamorphism

The Kazdağ Massif forms a 55 km long and 15 km wide NE-trending structural dome of gneiss, marble, amphibolite and meta-ultramafic rock. The meta-ultramafic rocks and metagabbro occur in the core of the dome enveloped by a marble-rich sequence, which passes up to felsic gneisses with marble and amphibolite intercalations (Bingöl, 1969; Pickett & Robertson, 1996). The depositional age of this series is not known owing to the lack of dateable fossils. On lithological, tectonic and metamorphic grounds, the Kazdağ Massif is correlated with the Rhodope crystalline complex in northern Greece and Bulgaria (Papanikolaou & Demirtaşlı, 1987). The western part the Kazdağ Massif consists of an intercalation of felsic gneiss, calc-silicate gneiss, amphibolite, marble with minor migmatite and metaserpentinite (Fig. 5).

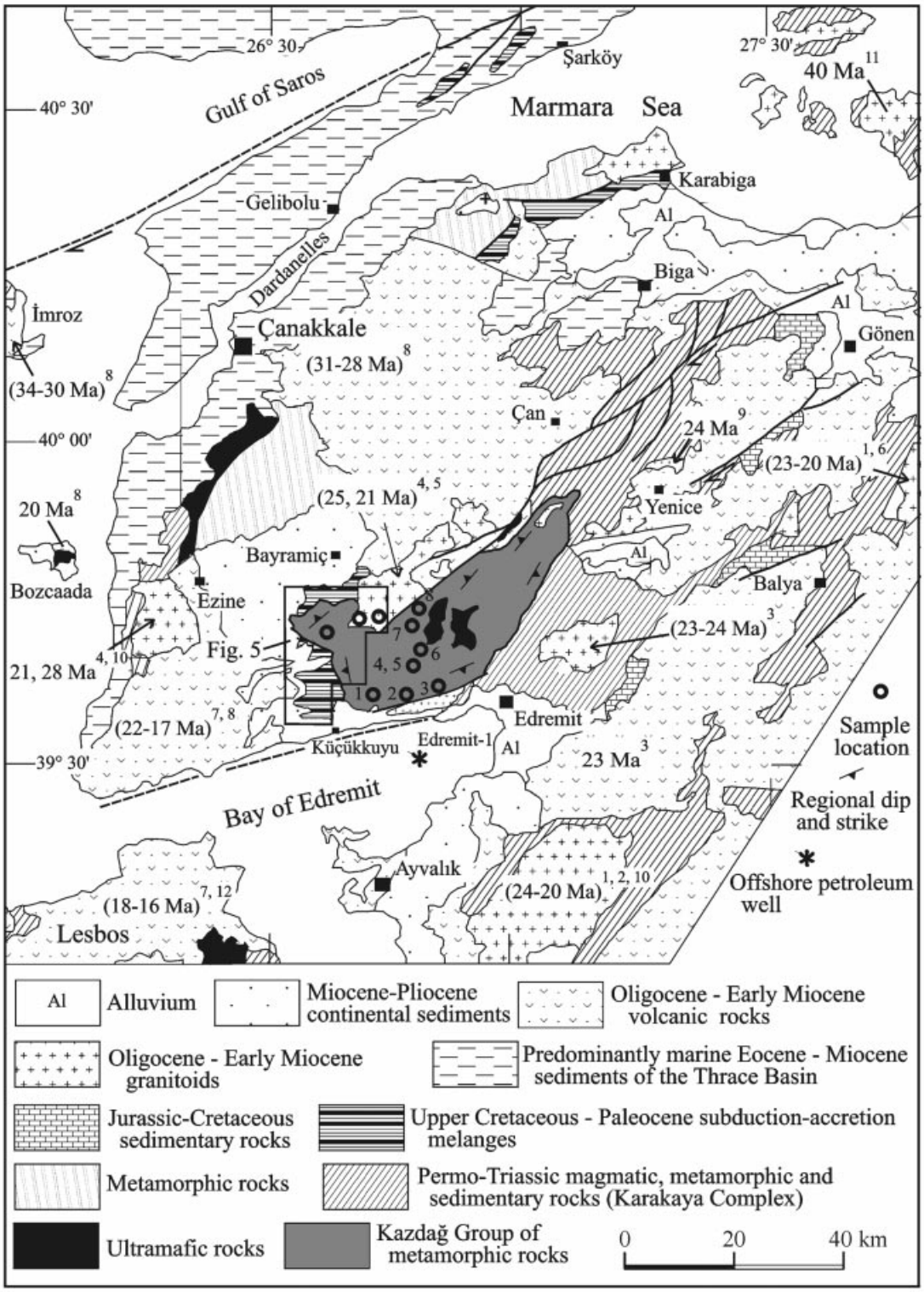

Figure 3. Geological map of northwestern Turkey illustrating the tectonic setting of the Kazdağ Massif and the isotopic ages of the Oligo-Miocene calc-alkaline magmatic province. The localities for the Rb/Sr geochronology are keyed to Table 3. Sources of the isotopic data (K/Ar and Rb/Sr) for the magmatic rocks are indicated by the superscripts: 1. Bingöl, Delaloye & Ataman (1982). 2. Ataman (1975). 3. Krushensky (1976). 4. Birkle & Satır (1995). 5. This study. 6. Ataman (1974). 7. Borsi *et al*. (1972). 8. Ercan *et al*. (1996). 9. Anıl *et al*. (1989). 10. Fytikas *et al*. (1976). 11. Bingöl *et al*. (1992). 12. Pe-Piper (1980).

The medium-grained gneisses are the most common lithology, making up ~60% of the outcrops. The marble forms one to 20 m thick horizons in the gneiss. Diopside-bearing amphibolites occur as bands, up to several metres thick, in the gneiss and marble.

3.a. Structure

The dominant structure in the Kazdağ Massif in the region studied is a compositional banding and foliation, which dip consistently northwest at ~ 35° (Fig. 6a)

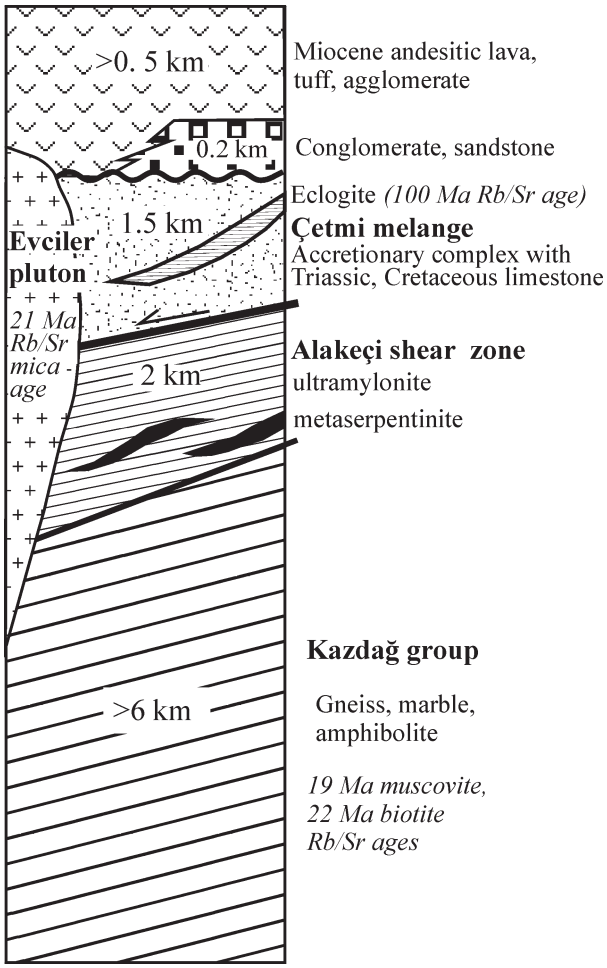

Figure 4. Columnar section showing the tectono-stratigraphic units in the western Kazdağ region.

resulting in a structural thickness of more than 5.5 km (Fig. 5). In the calc-silicate gneisses, the compositional banding is defined by millimetre- to centimetre-scale bands of alternating hornblende + plagioclase, and diopside + plagioclase + scapolite assemblages. The metamorphic rocks also show a weak mineral stretching lineation defined mainly by quartz and hornblende, which plunges north–northwest (~N33°W) at ~36° (Fig. 6b). Similar N-trending mineral lineations are described from other regions of the Kazdağ range (Schuiling, 1959; Bingöl, 1969; Sulzer, 1990). Rare folds are tight to isoclinal, rootless or with strongly attenuated limbs. The fold axial planes lie in the plane of the foliation and the fold axes parallel the lineation. Brittle structures in the metamorphic rocks include rare EW-trending normal faults with minor throws (<1 m).

Amphibolites and calc-silicates in the Kazdağ Massif have equant, granoblastic textures; in contrast, felsic gneisses generally show a mylonitic foliation defined by quartz ribbon formed through the recrystallization of quartz to flattened subgrains. The mylonitic foliation, which is parallel to the compositional banding, increases in intensity towards the top of the metamorphic sequence. Shear sense indicators, mainly shear band cleavage, mica fish, rotated mantled feldspars, rare in the bulk of the Kazdağ Massif, are well developed in this part. Out of six oriented thin sections of felsic gneiss sampled from the top 300 m of the metamorphic sequence, four contain down-dip, top-to-the-north shear sense indicators, while microfabrics in two sections are kinematically inconclusive. Without giving any details, Walcott & White (1998) also indicate top-to-the-north shear sense in the Kazdağ Massif. Sillimanite prisms and needles, which define a strong lineation even in the topmost part of the metamorphic sequence (Fig. 7b), indicate that the deformation was taking place during the peak metamorphism.

3.b. Petrology and *P–T* conditions

The Kazdağ Massif is metamorphosed in amphibolite facies with no noticeable change in the metamorphic grade across the area. The mineral assemblage in the felsic gneisses is quartz + plagioclase + biotite + muscovite ± garnet ± sillimanite (Fig. 7a,b). Garnet in felsic gneisses forms small resorbing grains, which display no zoning. They are essentially almandine–spessartine–pyrope solid solutions with minor grossular components (grossular < 7 mol.%); a typical composition is $grs_5pyr_{10}alm_{68}spess_{17}$. Sillimanite is closely associated with biotite and muscovite, and shows both fibrolitic and prismatic habits (Fig. 7a,b). Plagioclase is oligoclase to andesine with a restricted compositional range of $An_{26–36}$. The calc-silicate gneisses consist of quartz + plagioclase + diopside + hornblende ± garnet ± epidote ± scapolite. Between different calc-silicate samples, plagioclase shows a wide compositional variation ranging from oligoclase (an_{26}) to anorthite (an_{98}). Calcic amphiboles also show a range of chemical compositions among samples ranging from actinolite through actinolitic hornblende to magnesio-hornblende. Scapolites are rich in meionite component (77–80% meionite), which is typical of scapolites from high amphibolite and granulite facies terrains. Garnets from calc-silicate gneisses are almandine–grossular solid solutions with minor pyrope (<12 mol.%) and spessartine (<5 mol.%) contents. They show compositional zoning involving decreasing Fe/Mg ratio towards the rim at relatively constant or slightly decreasing grossular and spessartine contents. The common mineral assemblage in the amphibolites is plagioclase + hornblende + diopside ± epidote.

Three sillimanite-bearing felsic gneisses and three calc-silicate gneisses were analysed by a Camebax SX-50 electron microprobe to constrain the metamorphic pressures and temperatures. The felsic gneisses were analysed at Bureau de Recherches Geologiques et Minieres in Orleans, France, and the calc-silicate gneisses at the Ruhr-Universitat Bochum, Germany.

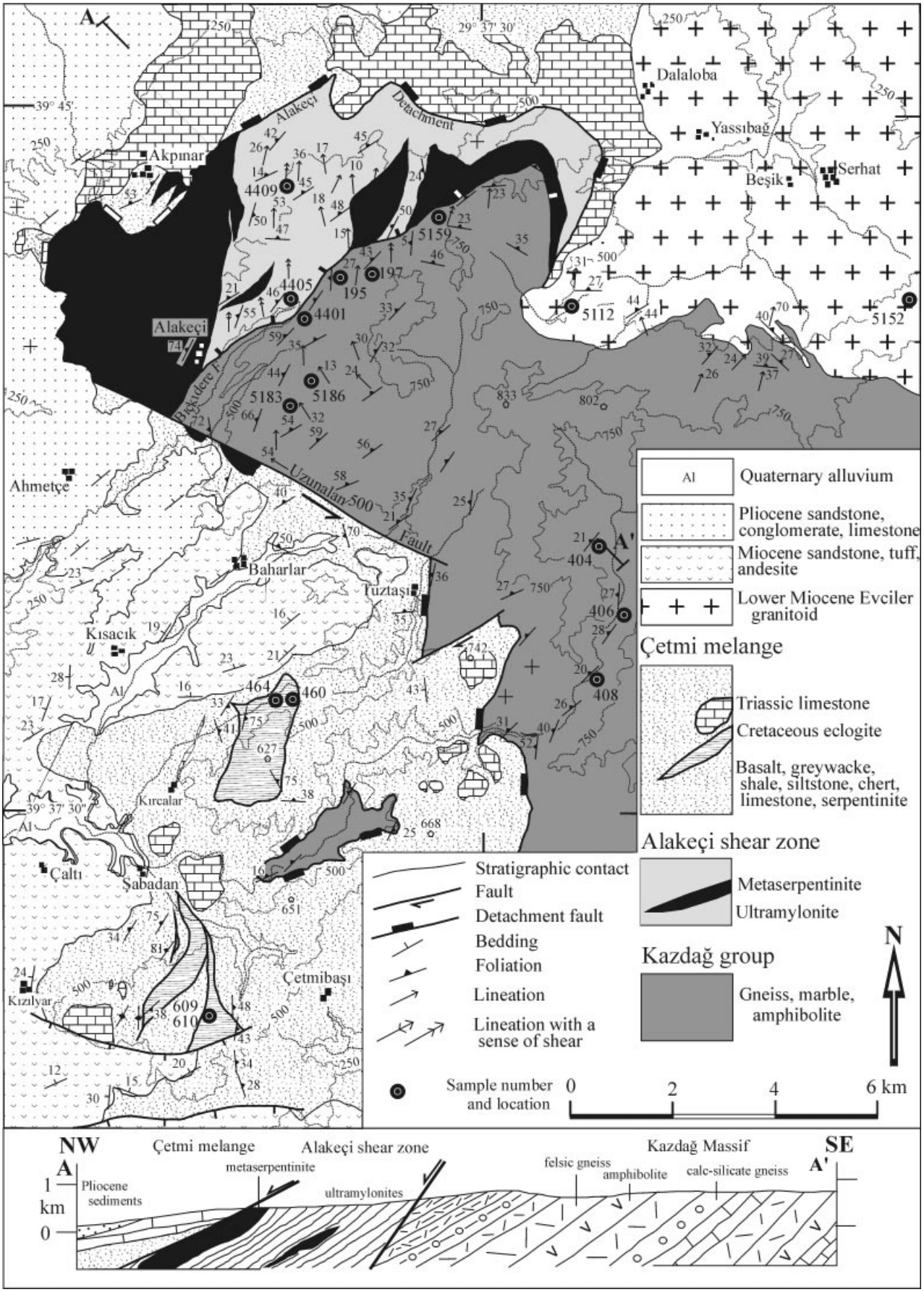

Figure 5. Geological map and cross-section of the western part of the Kazdağ range (modified after Okay, Siyako & Bürkan, 1991). For location see Figure 3. The contours are in metres.

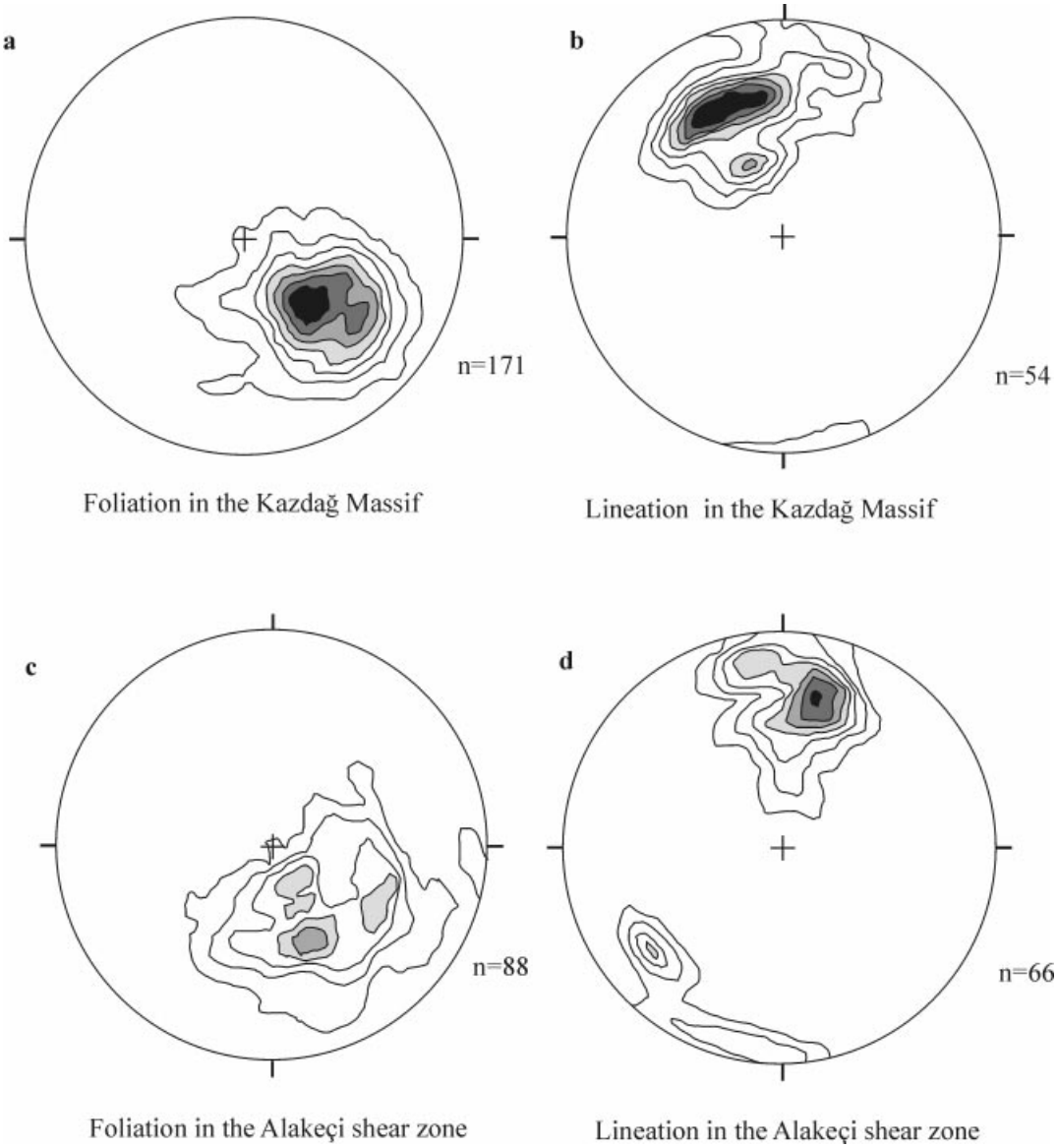

Figure 6. Lower hemisphere equal-area projections of foliation and lineation from the Kazdağ Massif and the Alakeçi shear zone. Contours are at 1, 3, 5, 7, 9, 11 and 13% per 1% area.

Operating conditions were 15 kV accelerating voltage, 10 or 15 nA beam current, and 10 μm beam size. The mineral modes and representative mineral compositions are given in Tables 1 and 2, respectively. The widely used garnet–sillimanite–plagioclase–quartz (GASP) geobarometer yielded pressures of 4 to 6 kbar at a temperature of 640°C for the three sillimanite-gneisses using the Koziol & Newton (1988) calibration (Fig. 8). A similar pressure range of 4.5 to 5.5 kbar at 640°C was obtained from two calc-silicate gneisses using the garnet–plagioclase–clinopyroxene–quartz geobarometer of Newton & Perkins (1982). Pressure estimates using the THERMOCALC program of Holland & Powell (1990) and the mineral chemical data from the three sillimanite-gneisses range from 4.5±1 kbar to 5.7±1 kbar at a temperature of 640°C. Unlike these relatively precise estimates of the metamorphic pressure, the metamorphic temperatures are less well constrained. The sillimanite + muscovite + quartz assemblage and absence of K-feldspar + sillimanite in the gneisses constrain the metamorphic temperatures between 585 and 690°C at 5 kbar (Fig. 8). The garnet–biotite geothermometer of Hodges & Spear (1982) gives temperatures of 560 to 615°C for the sillimanite-gneisses and ~650°C for the calc-silicate gneisses. The garnet–clinopyroxene geothermometer of Ellis & Green (1978) yielded temperatures of ~650°C for diopside and garnet pairs in the calc-silicate gneisses (Fig. 8). A reasonable estimate for the peak *P–T* conditions in the Kazdağ Massif are 5±1 kbar and 640°±50°C.

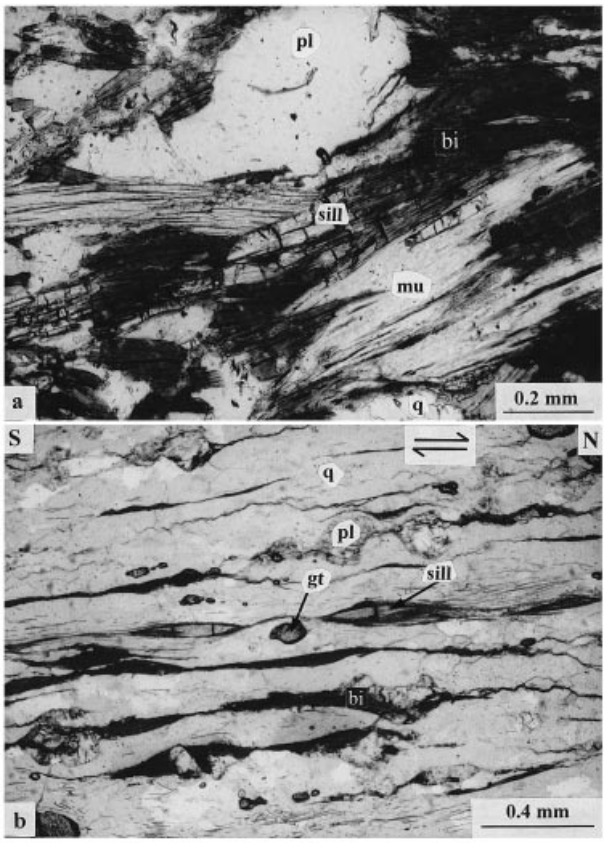

Figure 7. Photomicrographs in plane polarized light from the gneisses of the Kazdağ Massif. The location of the samples is shown in Figure 5. The deduced sense of shear and geographic directions are marked on the photomicrographs. Sections are parallel to the lineation and perpendicular to the foliation (a) Felsic gneiss (5183) with sillimanite (sill), muscovite (mu), biotite (bi), plagioclase (pl) and quartz. (b) High temperature mylonite (5159) from the topmost part of the Kazdağ Massif. The mylonite consists of sillimanite (sill), garnet (gt), biotite (bi), plagioclase (pl) and quartz (q). Sillimanite shows both prismatic and fibrolitic habits. The shear sense is given by the δ-type winged plagioclase porphyroclasts (top left), and biotite mica fish.

Table 1. Estimated modes of the analysed gneisses from the Kazdağ Massif

	Felsic gneiss			Calc-silicate gneiss			
Sample	4401	5183	5186	197B	404B	406B	408B
Quartz	64	31	33	64	11	17	30
Plagioclase	6	21	25	6	44	20	17
K-feldspar	–	–	–	5	–	3	3
Garnet	3	4	3	12	–	–	10
Biotite	17	35	28	–	–	19	19
Muscovite	7	4	6	–	–	–	2
Sillimanite	3	3	4	–	–	–	–
Diopside	–	–	–	4	23	17	11
Hornblende	–	–	–	2	15	11	7
Scapolite	–	–	–	5	–	12	–
Epidote	–	–	–	–	3	–	–
Titanite	–	–	tr	1	1	1	tr
Ilmenite	tr	2	1	–	–	–	tr
Magnetite	–	–	–	1	3	tr	1

tr, less than 0.5 %

3.c. Geochronology

Zircon ages from the Kazdağ gneisses, determined by single-zircon step-wise Pb-evaporation technique, are mid-Carboniferous (308 ± 16 Ma; Okay *et al.* 1996). Similar late Hercynian zircon and monazite ages are reported from the Rhodope Massif in Greece (Dinter *et al.* 1995; Wawrzenitz & Krohe, 1998). In the light of these regional tectonic data, the mid-Carboniferous ages from the Kazdağ Massif were previously interpreted as the age of Hercynian high-grade metamorphism (Okay *et al.* 1996). In contrast to these late Hercynian ages, Bingöl (1969) reported K–Ar mica ages of 26 ± 3 and 27 ± 3 Ma from two gneiss samples from the Kazdağ Massif. During this study nine gneiss samples from throughout the Kazdağ range (see Figs 3, 5 for the locations), including the two samples previously dated by zircons, were investigated by the Rb/Sr method. The Rb/Sr data are displayed in Table 3. The analytical procedures were the same as those described by Okay, Şengör & Satır (1993).

The biotite and muscovite Rb/Sr ages from the Kazdağ gneisses cluster between 20 and 18 Ma, and 24 and 20 Ma, respectively (Table 3). Two discrepancies are a muscovite age of 30 Ma from the sample 195B, and a 14 Ma biotite age from sample 1. In both of these samples the $^{87}Rb/^{86}Sr$ values of the micas are unusually low, and therefore, the age calculated is very sensitive to small errors in the initial $^{87}Rb/^{86}Sr$ ratio. If muscovite and biotite are used in the age calculation, rather than muscovite and whole rock, the Rb/Sr age of the sample 195B comes out to be 20.5 ± 0.4, similar to the muscovite and biotite ages from the other samples. The Rb–Sr system in this sample may also have been incompletely reset during the latest Oligocene metamorphism. In contrast, it is difficult to attach geological meaning to the 14 Ma biotite age from the gneiss, particularly since the Kazdağ metamorphic rocks are intruded by the Evciler granitoid, which has a 21 Ma biotite cooling age (see Section 6).

The closure temperatures of muscovite and biotite for Sr are generally considered to be ~500 °C and ~300 °C, respectively (e.g. Jäger, Niggli & Wenk, 1967; Cliff, 1985), although temperatures as high as 650 °C have been suggested for the closure of Sr in muscovite (cf. Villa, 1997). The average muscovite and biotite Rb/Sr ages from the Kazdağ gneisses are ~22 Ma and ~19 Ma, respectively. The closeness of the muscovite and biotite Rb/Sr ages suggests rapid cooling (~70 °C/m.y.), and assuming a similar cooling rate, indicates that the peak temperatures of 640 °C recorded in the metamorphic rocks were reached at ~24 Ma. With the Oligocene/Miocene boundary at 23.7 Ma (Berggren *et al.* 1985), this is latest Oligocene metamorphism. The muscovite and biotite Rb/Sr ages show a slight pattern of getting older towards the south (cf. Table 3 and Fig. 3), suggesting that the exhumation started in the south and progressed rapidly northward.

Table 2. Representative mineral compositions from the gneisses of the Kazdağ Massif

	Calc-silicate gneiss 408B							Calc-silicate gneiss 197B						Sillimanite-gneiss 4401				Sillimanite-gneiss 5186			
	Garnet							Garnet													
	Core	Rim	Biotite	Diop.	Plag.	K-feld	Hornbl.	Core	Rim	Diop.	Plag.	Actin.	Scapol.	Garnet	Musc.	Plag.	Biotite	Garnet	Musc.	Plag.	Biotite
SiO_2	36.89	37.16	35.35	51.24	54.66	63.73	45.47	37.11	37.31	51.11	46.42	51.52	44.51	38.85	45.91	59.56	35.27	38.99	45.18	59.25	35.62
TiO_2	0.11	0.17	3.48	0.15	0.05	0.00	0.50	0.04	0.00	0.01	0.00	0.03	0.00	0.00	0.76	0.00	2.21	0.00	0.81	0.00	2.69
Al_2O_3	20.89	21.33	15.24	1.08	28.20	18.60	8.89	21.17	21.22	0.41	32.93	2.75	27.17	22.04	36.06	25.53	20.56	22.06	36.3	26.06	20.76
Cr_2O_3	0.11	0.03	0.15	0.10	0.00	0.00	0.19	0.00	0.02	0.00	0.01	0.00	0.00	0.07	0.00	0.01	0.11	0.00	0.22	0.07	0.00
FeO	22.17	28.36	19.39	10.82	0.32	0.06	16.91	15.23	15.84	11.45	0.07	12.81	0.05	30.87	1.04	0.01	17.85	29.52	1.02	0.07	18.90
MgO	0.97	2.48	10.49	11.07	0.00	0.01	10.06	2.49	1.99	10.36	0.01	14.50	0.01	2.44	0.57	0.00	8.97	2.33	0.57	0.00	8.62
MnO	7.39	1.08	0.29	0.26	0.00	0.03	0.32	8.77	8.87	1.43	0.01	0.69	0.00	8.09	0.04	0.00	0.05	8.43	0.06	0.00	0.41
CaO	10.39	9.18	0.16	23.53	10.99	0.03	12.00	14.22	13.43	23.85	17.69	13.23	18.22	1.46	0.00	6.71	0.00	2.04	0.00	7.14	0.00
Na_2O	0.01	0.03	0.13	0.24	5.39	0.77	0.89	0.01	0.02	0.13	1.94	0.24	3.05	0.03	0.81	8.03	0.20	0.04	0.61	7.37	0.13
K_2O	0.02	0.01	9.62	0.02	0.21	15.45	0.92	0.00	0.00	0.02	0.05	0.16	0.09	0.00	9.78	0.13	8.65	0.02	9.95	0.16	9.37
Cl	nd	nd	0.22	nd	nd	nd	0.06	nd	nd	nd	nd	0.00	0.11	nd	nd	nd	nd	nd	nd	nd	nd
F	nd	nd	0.20	nd	nd	nd	0.06	nd	nd	nd	nd	0.24	nd	0.00	0.00	0.00	0.33	0.00	0.00	0.22	0.00
Total	98.96	99.84	94.73	98.50	99.83	98.67	96.26	99.04	98.69	98.79	99.13	96.17	93.21	103.84	98.69	99.97	97.61	103.42	98.44	100.29	96.59
Mineral formula on the basis of																					
	12 O	12 O	11 O	6 O	8 O	8 O	23 O	12 O	12 O	6 O	8 O	23 O	12 (Si,Al)	12 O	11 O	8 O	11 O	12 O	11 O	8 O	11 O
Si	2.981	2.960	2.747	1.972	2.474	2.981	6.884	2.944	2.976	1.980	2.159	7.628	6.979	3.015	3.051	2.657	2.688	3.028	3.017	2.640	2.664
Al_{IV}	0.019	0.040	1.253	0.028	1.505	1.025	1.116	0.056	0.024	0.019	1.805	0.372	5.021	0.949	1.342	1.313	0.983	1.368	1.337		
Al_{VI}	1.971	1.962	0.143	0.021	0.470	1.923	1.970	0.109	2.015	1.876	0.533	2.019	1.875	0.493							
Ti	0.006	0.010	0.204	0.004	0.002	0.000	0.057	0.002	0.000	0.000	0.000	0.004	0.000	0.000	0.038	0.000	0.127	0.000	0.041	0.000	0.151
Cr	0.007	0.002	0.010	0.003	0.000	0.000	0.022	0.000	0.001	0.000	0.001	0.000	0.000	0.004	0.000	0.000	0.006	0.000	0.011	0.000	0.000
Fe^{3+}	0.016	0.026	0.011	0.002	0.018	0.075	0.029	0.002	0.000	0.006	0.000		0.000								
Fe^{2+}	1.482	1.863	1.260	0.348	2.123	0.935	1.028	0.371	1.587	2.003	0.058	1.138	1.917	0.057	1.182						
Mg	0.117	0.294	1.215	0.635	0.000	0.001	2.269	0.294	0.236	0.598	0.001	3.199	0.002	0.282	0.057	0.000	1.018	0.270	0.057	0.000	0.961
Mn	0.506	0.073	0.019	0.008	0.000	0.001	0.041	0.589	0.600	0.047	0.000	0.087	0.000	0.532	0.002	0.000	0.003	0.555	0.003	0.000	0.026
Ca	0.899	0.783	0.013	0.970	0.533	0.001	1.954	1.208	1.147	0.990	0.881	2.099	3.061	0.121	0.000	0.321	0.000	0.170	0.000	0.341	0.000
Na	0.002	0.004	0.020	0.018	0.473	0.070	0.263	0.002	0.003	0.010	0.175	0.069	0.928	0.004	0.105	0.695	0.029	0.005	0.079	0.637	0.020
K	0.002	0.001	0.953	0.011	0.012	0.922	0.178	0.000	0.000	0.001	0.003	0.030	0.017	0.000	0.829	0.007	0.841	0.002	0.848	0.009	0.894
Total	8.008	8.018	7.837	4.018	5.010	5.003	15.395	8.028	8.014	4.016	5.027	15.184	16.014	7.976	6.965	5.022	7.696	7.966	6.971	4.995	7.728
alm	49.3	61.8					alm	30.9	34.1				alm	68.2			alm	65.9			
pyr	3.9	9.8		an	52.4	0.1	pyr	9.7	7.8				pyr	9.6	an	31.4	pyr	9.3	an	34.6	
spess	16.8	2.4		ab	46.5	7.1	spess	19.5	19.9				spess	18.1	ab	67.9	spess	19.1	ab	64.5	
gros	29.1	24.7		or	1.2	92.8	gros	36.2	36.7				gros	3.9	or	0.7	gros	5.8	or	0.9	
andr	0.8	1.3					andr	3.8	1.4				andr				andr				

nd, not determined

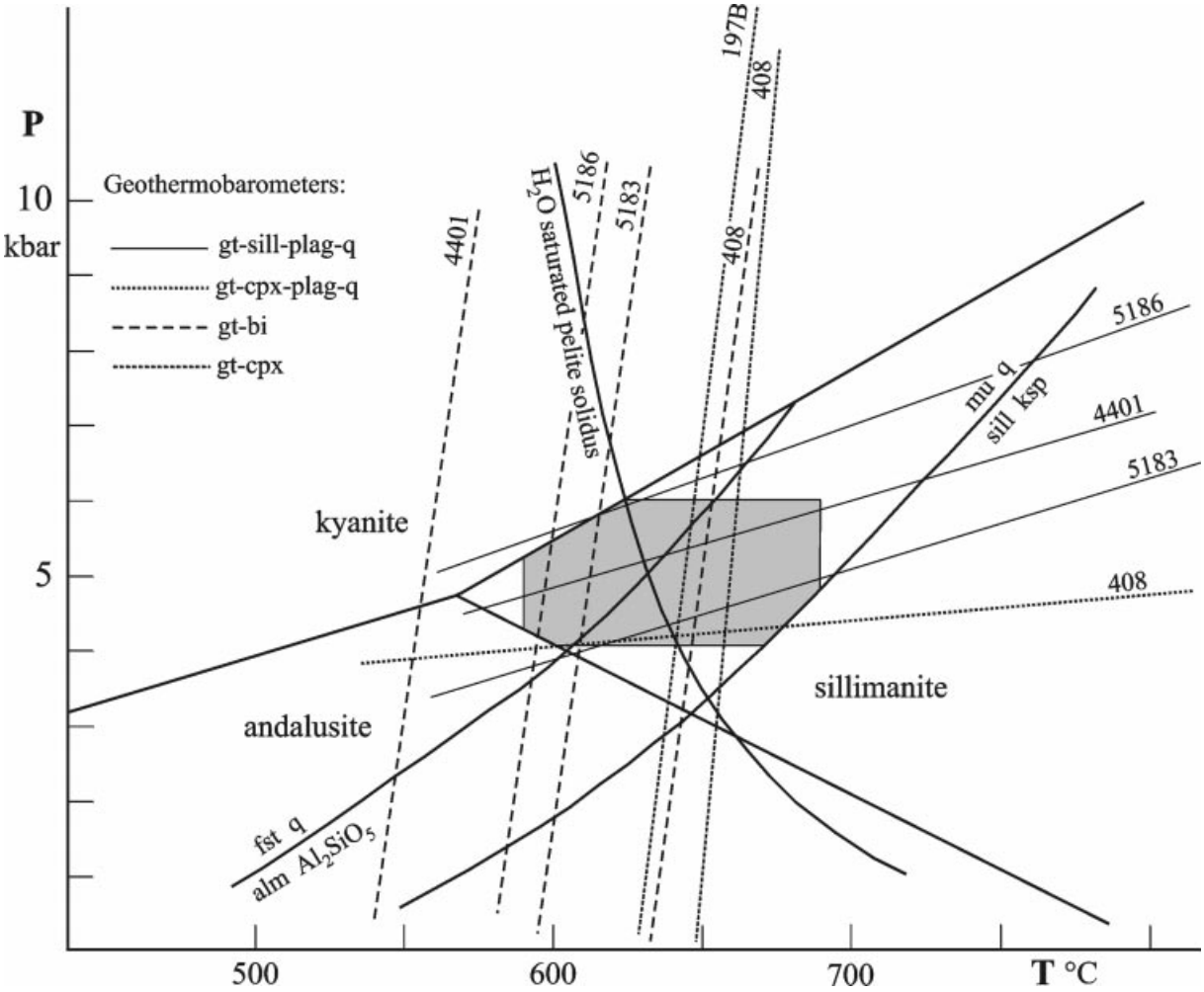

Figure 8. Pressure–temperature diagram illustrating the estimated *P–T* conditions of metamorphism and the relevant equilibria in the Kazdağ Massif. The end-member reactions are from the THERMOCALC program of Holland & Powell (1990). For the various geothermobarometers see the text. Abbreviations: alm, almandine; bi, biotite; cpx, clinopyroxene; fst, ferrostaurolite; gt, garnet; ksp, K-feldspar; mu, muscovite; plag, plagioclase; q, quartz; sill, sillimanite.

3.d. Carboniferous or latest Oligocene metamorphic mineral assemblages?

The petrography of the Kazdağ metamorphic rocks in the region studied indicates a single high temperature metamorphic event. The age of this amphibolite facies mineral assemblage, whether Carboniferous as indicated by the zircons, or latest Oligocene as shown by the mica Rb/Sr ages, is an important problem. The muscovite Rb/Sr cooling ages from the Kazdağ Massif indicate that the temperatures in the metamorphic rocks during the latest Oligocene were above 500 °C. The foliation and lineation in the metamorphic rocks are subparallel to those in the Alakeçi shear zone and to the foliation and lineation in the latest Oligocene Evciler granitoid (see Section 6). This suggests that the metamorphic minerals, such as biotite, muscovite, sillimanite and garnet, which define the structural fabric in the Kazdağ gneisses, were formed or reoriented during latest Oligocene times. Sillimanite needles aligned to the lineation in the plastically deformed quartz ribbons (Fig. 6b) indicate that they grew rather than rotated during latest Oligocene times. Hence, the mineral assemblages in the Massif must have formed during this period. This is in contrast to earlier views, which regarded the Kazdağ Massif as a Hercynian metamorphic unit (e.g. Schuiling, 1959; Brinkmann, 1976; Okay *et al.* 1996). The late Hercynian metamorphic rocks were presumably completely recrystallized during the latest Oligocene with only the zircons retaining a memory of the older metamorphic event.

4. Alakeçi shear zone

A shear zone of strongly mylonitized gneiss and serpentinite, two kilometres in thickness, occurs between the Kazdağ Massif and the accretionary melange in the north (Okay, Siyako & Bürkan, 1991) (Figs 4, 5). The mylonites show a well-developed mineral lineation defined by quartz, mica and amphibole, which plunges north–northeast (~N12°E) at

Table 3. Rb/Sr isotopic data from the Kazdağ region

Sample	Mineral	Rb, ppm	Sr, ppm	$^{87}Rb/^{86}Sr$	$^{87}Sr/^{86}Sr$	Age, Ma
Kazdağ gneisses						
1	rock	27	86	0.91	0.708075	
	biotite	401	9.89	118	0.728979	14 ± 0.1
2	rock	125	140	2.59	0.719144	
	muscovite	366	10.22	104.0	0.752084	23 ± 0.2
3	rock	141	125	3.27	0.724328	
	muscovite	428	13.09	95.1	0.756055	24 ± 0.3
4	rock	68	143	1.38	0.714796	
	biotite	362	2.28	466	0.841167	19 ± 0.2
5	rock	79	112	2.04	0.716478	
	muscovite	363	9.77	108	0.747145	20 ± 0.2
6	rock	73	237	0.89	0.714226	
	muscovite	187	24.27	22.3	0.720344	20 ± 0.2
	biotite	367	3.40	315	0.796095	18 ± 0.2
7	rock	102	164	1.80	0.718284	
	biotite	475	2.27	616	0.887441	19 ± 0.2
8	rock	152	100	4.41	0.728559	
	biotite	646	1.77	1090	1.012891	18 ± 0.2
195B	rock	56	575	0.282	0.70693	
	muscovite	207	93.2	6.427	0.70952	30 ± 0.4
	biotite	433	12	104.69	0.73701	20 ± 0.2
	plagioclase	12.5	628	0.058	0.70679	
Elliayak eclogite						
609D	rock	68.6	139.0	1.428	0.710306	
	phengite	247.9	74.0	9.705	0.722099	100.3 ± 2.8
457A	rock	65.46	158.6	1.194	0.709252	
	phengite	337.3	209.0	4.672	0.714154	99.0 ± 6.1
Evciler granitoid						
5112	rock	59	492	0.35	0.705711	
	biotite	354	6	160	0.752677	20.7 ± 0.2
	cpx	1.9	24.5	0.23	0.705697	
5151	rock	156	463	0.98	0.710112	
	biotite	773	5	456	0.842671	20.5 ± 0.2
	hornblende	11.5	229	0.15	0.709716	

~30° (Fig. 6d). The foliation, which is deflected around the large serpentinite bodies, is more scattered but shows a general northwestward dip (Fig. 6c). The protoliths of the mylonites were largely the felsic gneisses of the Kazdağ Massif. They consist mainly of very fine-grained (<0.1 mm) quartz, plagioclase, biotite and chlorite, which show a sub-millimetric mylonitic foliation (Fig. 9). Quartz locally forms ribbons up to 1 mm long and less than 0.1 mm wide. The porphyroclasts are rare, and include garnet and plagioclase. Amphibolites and marbles form boudins within the felsic mylonites. In the centre of the shear zone the ultramylonites are strongly sericitized. Antigorite-serpentinites occur as lenses, ranging in length from 10 cm to 4 km, in the mylonite; they are probably derived from the metadunites, which are interfolded with the marble and gneiss in the central part of the Kazdağ range (Fig. 3). The protoliths of some mylonites, that contain large plagioclase porphyroclasts in a very fine grained matrix, may have been subvolcanic rocks. Seven oriented samples were collected from the Alakeçi shear zone. Shear sense indicators, mainly rotated mantled feldspars (Fig. 9a), C'-type shear band cleavage (Fig. 9b), and mica fish, in four thin sections show down-dip, top-to-the-north shear sense, in two sections top-to-the-south shear sense, and one is inconclusive.

The Alakeçi fault constitutes the upper contact of the shear zone. Along the Alakeçi fault, mafic volcanic rocks showing a rough, spaced foliation lie over the mylonite or serpentinite. The dip of the Alakeçi fault is ~30° in the west; it increases towards the east as a result of the igneous intrusion and becomes subvertical around the Evciler pluton. The fault plane is not planar but on map view shows NNE-dipping corrugations, a feature observed in many detachment faults (e.g. Dinter & Royden, 1993). The Alakeçi fault is interpreted as a low-angle detachment, which juxtaposes brittlely deformed upper crustal rocks over the ductilely deformed mid-crustal rocks.

The Bıçkıdere fault forms the contact between the Kazdağ Massif and the shear zone. It is characterized by brecciation of the overlying ultramylonites. The most striking difference across the Bıçkıdere fault is reduction in the grain size, from 0.5–1 mm in the gneisses below the fault to less than 0.1 mm above, coupled with a distinct increase in the intensity of lineation. The Bıçkıdere fault dips at 55° to the northwest and is steeper than the regional foliation on either side (Fig. 5).

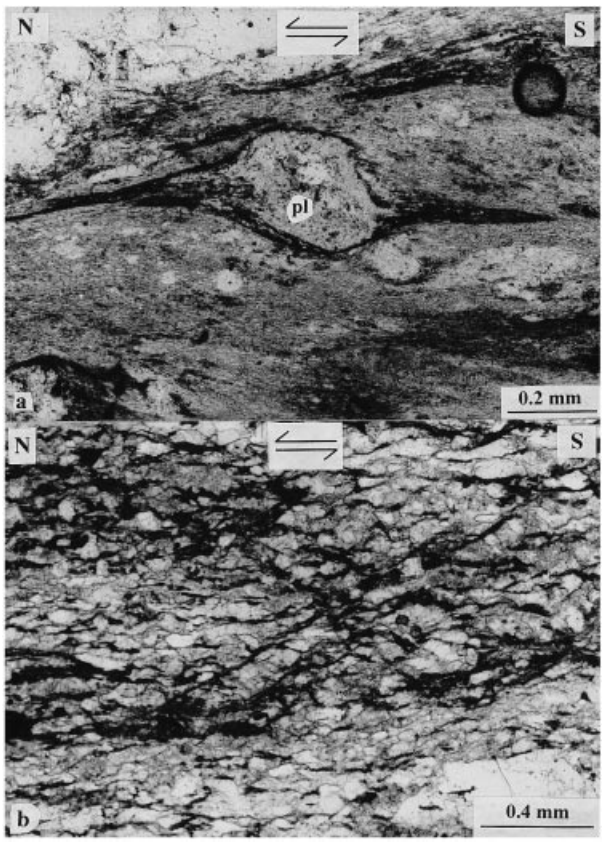

Figure 9. Photomicrographs in plane polarized light from the Alakeçi shear zone. The deduced sense of shear and geographic directions are marked on the photomicrographs. Sections are parallel to the lineation and perpendicular to the foliation. The location of the samples is shown in Figure 5. (a) Mylonite (4409) with a σ-type winged plagioclase porphyroclast in a fine grained matrix of sericitic white mica, biotite, feldspar and quartz. The 'wings' of the porphyroclast consist of biotite and feldspar. (b) C'-type shear band cleavage (from upper right to lower left) in the mylonite (4405) of feldspar, quartz and mica. Biotite has concentrated along the shear cleavages, which lie at an angle of ~33° to the mylonitic foliation.

Table 4. Estimated modes of the analysed eclogites and eclogitic micaschists

	Eclogite				Micaschist	
Sample	460	464	610B	610E	609A	609D
Garnet	27	45	21	41	11	9
Omphacite	31	33	32	8	–	–
Glaucophane	33	–	19	29	–	11
White mica	1	–	12m	9m	26m,p	22p
Epidote	–	4	9	5	–	18
Clinozoisite	–	13	–	tr	–	–
Quartz	4	–	5	4	55	35
Rutile	4	1	2	3	tr	tr
Opaque	tr_{pyr}	–	–	–	tr	2
Chlorite	–	2	tr	1	tr	3
Albite	–	2	–	–	–	–
Graphite	–	tr	–	–	–	–
Titanite	–	–	–	–	–	tr
Calcite	–	–	tr	tr	–	–
Ankerite	–	–	–	–	8	–

tr, less than 0.5 %; m, phengite; p, paragonite; pyr, pyrite

Minimum and maximum pressures for the mylonites in the shear zone are provided by the estimated depth of emplacement of the Evciler pluton (~3 kbar, see Section 6) and by the *P–T* conditions of the latest Oligocene regional metamorphism in the Kazdağ Massif (~5 kbar). The mineral assemblage in the ultramylonites, quartz + plagioclase + biotite ± garnet, indicates upper greenschist-facies *P–T* conditions, which is compatible with the thermal stability limit of antigorite (275–500 °C: Evans, 1977) in the shear zone. Prior to the inception of the Bıçkıdere fault, there must have been a continuous gradation from the metamorphic rocks of the Kazdağ Massif at the base to the ultramylonites at the top of the sequence.

Two lines of evidence indicate that the Alakeçi shear zone is dominantly of extensional origin: (1) it juxtaposes unmetamorphosed shallow crustal rocks in the hangingwall upon mid-crustal high-grade metamorphic rocks in the footwall (Okay, Siyako & Bürkan, 1991); (2) kinematic indicators in the shear zone and in the footwall mylonites exhibit predominantly a north-directed down-dip or normal sense of shear relative to the present orientation of the mylonitic foliation. However, the lineation in the mylonites is slightly oblique to the boundaries of the shear zone (Figs 5, 6). This observation and the *en echelon* arrangement of the serpentinite bodies within the shear zone suggest a variable dextral strike-slip component of the down-dip extension. This view is further supported by the clockwise rotation of the azimuth of the lineations from the Kazdağ Massif (average N33°W) to the Alakeçi shear zone (N12°E).

The Alakeçi shear zone is sharply truncated in the south by a WNW-trending fault (Fig. 5). The steep southward dip (~75°) of this Uzunalan fault, as well as the offset along it, indicate that it is a sinistral transtensional strike-slip fault. South of the Uzunalan fault, the Çetmi accretionary melange rests directly on the Kazdağ Massif along a brittle fault plane. This fault plane dips ~25° west and is underlain by 150 m thick cataclastic gneiss. It is interpreted as a low-angle normal fault, which has cut out the Alakeçi shear zone. It is probably genetically related to the Bıçkıdere fault, whose steep dip would result in the omission of the shear zone at higher structural levels (cf. cross-section in Fig. 5).

The throw along the Alakeçi fault can be estimated from the known stratigraphy of northwest Turkey. The Kazdağ Massif is tectonically overlain in the east by the various units of the Permo-Triassic Karakaya Complex, with a minimum thickness of ~5 km (Okay *et al.* 1996). The Jurassic–Palaeocene sedimentary rocks, which lie unconformably over the Karakaya Complex, attain a thickness of ~1.5 km. The accretionary melange would be expected to lie tectonically

above the Late Cretaceous to Palaeocene carbonates. Thus, a section at least 6.5 km thick is omitted along the Alakeçi fault. The difference between the peak pressure of the regional metamorphism of the footwall gneisses (5 ± 1 kbar) and that of the emplacement of the Evciler granite (2.6 ± 1 kbar, see Section 6) also gives a similar amount of excision on the contact. Most of the strain during the extensional deformation appears to have been localized in the Alakeçi shear zone, however, the weak N-trending mineral lineation throughout the Kazdağ Massif shows that some of the strain may also have been distributed through the Kazdağ Massif.

5. Çetmi accretionary melange: hangingwall with eclogite blocks

The Çetmi accretionary melange consists mainly of spilitized mafic volcanic rocks (~45%), various types of limestone (~32%), greywacke-shale (~15%) with minor radiolarian chert and serpentinite, and large tectonic slices of eclogite and eclogitic micaschist (Fig. 5). A tectonic window of the Kazdağ Massif in the Çetmi melange (Fig. 5) indicates that the vertical structural thickness of the melange does not exceed 1.5 km. The rocks in the melange, apart from the eclogites and associated schists, are unmetamorphosed and generally do not show a penetrative foliation. Different lithologies cannot be traced for more than a few hundred metres along strike before they show faulted and sheared contacts; the whole complex has a melange-like character, however, it is difficult to define a single all-encompassing matrix. The mafic volcanic rocks form agglomerates and pillow lavas. The various limestone blocks include pelagic and neritic Upper Triassic, and pelagic Upper Cretaceous limestones, as well as recrystallized carbonate blocks. The carbonate blocks exhibit faulted contacts with the surrounding mafic volcanic rocks. The pelagic Triassic limestone blocks, which range up to one kilometre in size, consist of thinly bedded radiolarian micrites with the characteristic Norian (Upper Triassic) pelagic bivalve *Monotis salinaria.* They also contain Norian foraminifera of *Trochommina* sp., *Agathammina austroalpina*, *Galeanella* cf. *panticae*, *Nodosaria* sp., *N. ordinata*, *Austrocolomia* sp., *Aulotortus* spp., *A. gaschei*, *A. communis*, *A.* gr. *sinousus*, *Spiroamphorella carpathica*. The neritic Upper Triassic limestone blocks, which are up to two kilometres in size, are thickly bedded to massive biorudites with the abundant Upper Triassic bivalve *Megaladont* sp. The Upper Cretaceous limestones occur as rare, several-metre-size, red silty biomicrites in Couches-Rouges facies embedded in a greywacke–shale matrix. They yield Turonian–Santonian pelagic foraminifera of *Marginotruncana* sp., *M. coranata*, *M. marginata*, *M.* cf. *pseudolineiana* (Brinkmann *et al.* 1977; Okay, Siyako & Bürkan, 1991).

5.a. Eclogite blocks in the Çetmi melange

Two exotic blocks of eclogite and enclosing micaschist, 2–3 km long and less than 1 km wide, occur in the Çetmi accretionary melange (Fig. 5). The garnet-micaschists form silvery grey, well-foliated, homogeneous rocks with mesoscopic garnet porphyroblasts. The mineral assemblage in the garnet-micaschists is garnet + quartz + phengite + paragonite. The garnet-micaschists comprise 0.2–20 m thick horizons of eclogites, which are variably altered to blueschists. The eclogites are greenish, massive, dense, banded rocks with the mineral assemblage of garnet + omphacite + sodic amphibole + epidote + phengite + rutile ± quartz (Table 2). There is a continuous petrographic range from essentially anhydrous eclogite to a blueschist metabasite with garnet and sodic amphibole but no omphacite. Foliation and greenschist-facies mineralogy have developed in mafic volcanic rocks along a hundreds-of-metres thick contact zone of the eclogite–micaschist bodies.

Four eclogite and two eclogitic micaschist samples were analysed with a Camebax SX-50 electron microprobe at the Ruhr-Universität Bochum. Operating conditions were 15 kV accelerating voltage, 10 or 15 nA beam current, and 10 μm beam size. The estimated modes and representative mineral compositions are given in Tables 4 and 5, respectively. In the eclogites garnet, omphacite and glaucophane make up over 70% of the rock. Garnet forms subidioblastic crystals 2–4 mm in size with quartz, rutile and glaucophane inclusions and is essentially almandine–grossular solid solution with minor pyrope (3–11 mol.%) and spessartine (0–4 mol.%) (Table 5, Fig. 10a). Sodic amphibole occurs as prismatic, lavender blue crystals as large as 4 mm. It has rims and patches of bluish-green barroisite but otherwise is compositionally homogeneous and plots in the glaucophane and crossite fields (Fig. 10c). Apple-green omphacite crystals as long as 2 mm commonly occur as inclusions in glaucophane as well as in the matrix of the rock. Omphacite contains up to 36 mol.% jadeite and 15–25 mol.% aegirine (Table 5, Fig. 10b). Epidote is found as aggregates of grains 0.2 mm in size. Phengite with 3.30–3.45 Si per formula unit (Fig. 10d) is present in only one sample as grains 0.4–1 mm across associated with garnet. Phengite grains show a slight rimward decrease in Si. However, the compositional variation between grains is larger than that introduced by zoning. The greenschist-facies overprint in the eclogite is characterized by barroisite rims around glaucophane, the development of interstitial albite, and the partial replacement of garnet by chlorite.

Garnet–clinopyroxene Fe–Mg geothermometry of Ellis & Green (1979) indicates temperatures of 480 ± 50 °C at a pressure of 10 kbar for adjoining omphacite–garnet pairs from the eclogite samples, whereas minimum pressure of 10 kbar can be

Table 5. Representative mineral compositions from the eclogites and eclogitic micaschist

	Garnet						Amphibole	Omphacite		Epidote		Phengite		Paragonite
	464		609A		610B									
	Core	Rim	Core	Rim	Core	Rim	610B	464	610B	464	610B	609A	610B	609A
SiO_2	36.95	37.68	37.00	37.59	36.80	37.49	55.94	55.46	54.67	38.99	37.11	49.21	48.82	47.01
TiO_2	0.05	0.14	0.10	0.05	0.14	0.11	0.02	0.06	0.05	0.08	0.06	0.27	0.26	0.09
Al_2O_3	20.86	21.07	20.91	21.43	20.34	21.00	9.05	11.51	9.03	31.82	25.45	29.06	25.94	39.79
Cr_2O_3	0.03	0.03	0.02	0.02	0.07	0.03	0.03	0.02	0.00	0.04	0.04	0.03	0.06	0.00
FeO	27.82	23.95	31.22	25.74	30.47	27.76	13.50	4.51	7.54	1.03	9.01	2.12	2.88	0.40
MgO	1.55	2.87	1.69	2.66	2.37	4.86	9.21	7.12	7.46	0.02	0.18	2.60	3.51	0.11
MnO	1.36	0.70	1.32	0.63	0.57	0.36	0.07	0.05	0.03	0.01	0.01	0.00	0.05	0.00
CaO	10.24	12.57	7.53	11.17	8.43	7.51	1.01	12.93	12.28	23.35	22.80	0.00	0.00	0.19
Na_2O	0.03	0.00	0.03	0.00	0.03	0.03	6.87	6.83	7.06	0.00	0.00	0.57	0.64	6.85
K_2O	0.01	0.01	0.02	0.00	0.01	0.00	0.03	0.01	0.03	0.01	0.00	9.54	10.30	0.91
Total	98.91	99.01	99.84	99.29	99.23	99.15	95.73	98.50	98.15	95.34	94.66	93.40	92.46	95.35
Mineral formula on the basis of														
	12 oxygens						23 oxygens	4 cations		8 cations		11 oxygens		
Si	2.979	2.985	2.979	2.984	2.964	2.968	7.904	2.004	1.994	3.044	2.987	3.330	3.380	2.999
AlIV	0.021	0.015	0.021	0.016	0.036	0.032	0.096	0.000	0.006	2.928	0.013	0.670	0.620	1.001
AlVI	1.961	1.953	1.963	1.990	1.928	1.928	1.410	0.491	0.382		2.400	1.648	1.498	1.991
Ti	0.007	0.008	0.006	0.002	0.008	0.007	0.002	0.002	0.001	0.004	0.004	0.014	0.014	0.004
Cr	0.004	0.002	0.002	0.002	0.004	0.002	0.003	0.001	0.000	0.002	0.002	0.002	0.004	0.000
Fe^{3+}	0.028	0.037	0.029	0.006	0.060	0.063	0.568	0.000	0.098	0.068	0.606			
Fe^{2+}	1.848	1.513	2.074	1.702	1.900	1.712	1.027	0.136	0.132			0.120	0.166	0.021
Mg	0.186	0.340	0.203	0.315	0.284	0.574	1.940	0.383	0.406	0.002	0.022	0.263	0.362	0.012
Mn	0.093	0.047	0.090	0.042	0.039	0.025	0.008	0.002	0.001	0.000	0.000	0.000	0.004	0.000
Ca	0.885	1.067	0.650	0.950	0.728	0.637	0.153	0.501	0.500	1.952	1.965	0.000	0.000	0.013
Na	0.005	0.000	0.004	0.000	0.005	0.005	1.883	0.479	0.480	0.000	0.000	0.075	0.086	0.847
K	0.001	0.001	0.002	0.000	0.001	0.000	0.005	0.001	0.001	0.000	0.000	0.824	0.910	0.075
Total	8.018	7.968	8.023	8.009	7.957	7.953	14.999	4.000	4.001	8.000	8.000	6.946	7.044	6.963
alm	61.4	51.6	68.7	56.6	65.1	59.0	jd	49.1	38.2					
pyr	6.2	11.3	6.7	10.5	9.4	19.1	aeg	0.0	9.8					
spess	3.1	1.6	3.0	1.4	1.3	0.8	aug	50.9	52.0					
gros	29.4	35.5	21.6	31.6	24.2	21.2								

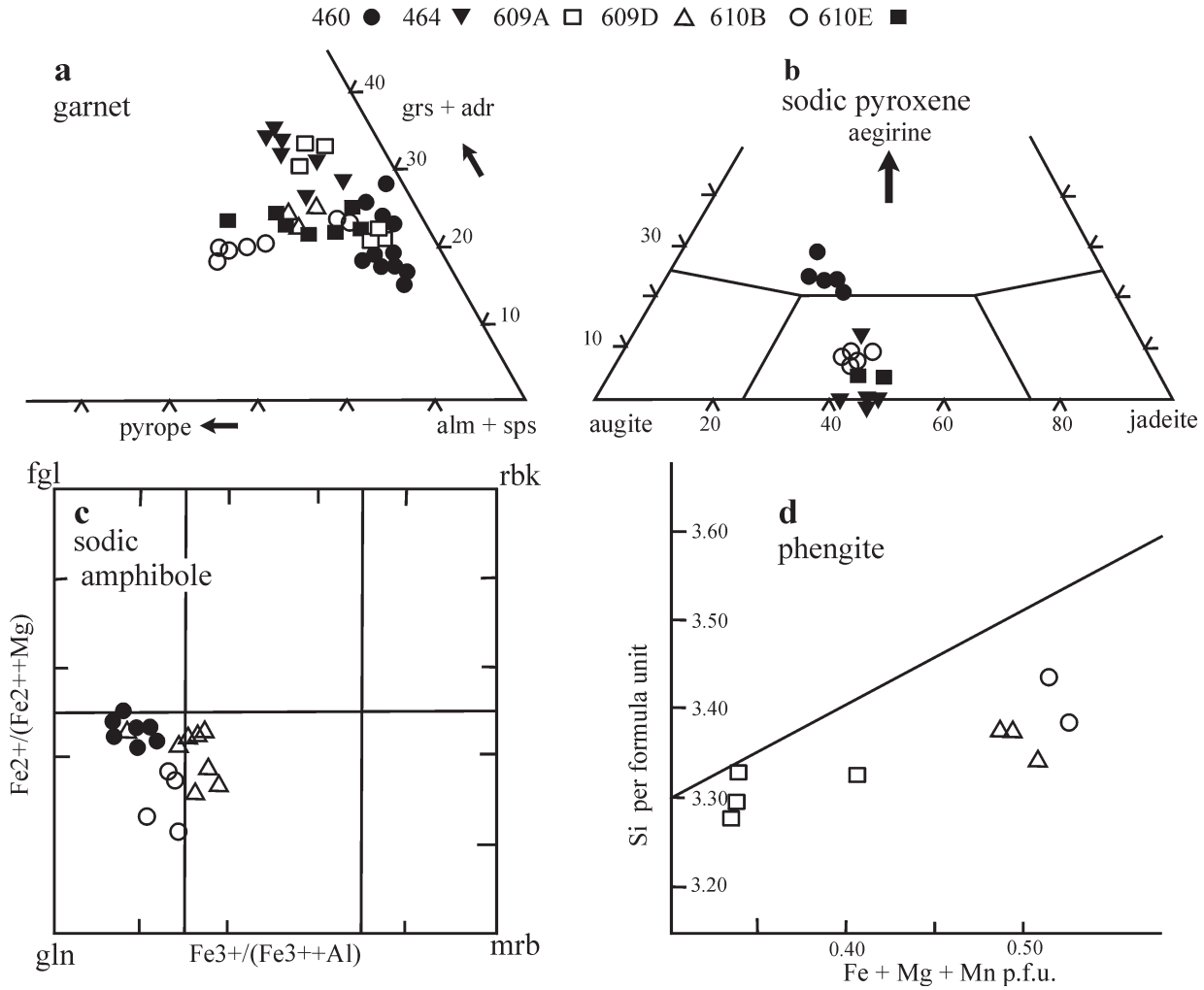

Figure 10. Garnet, sodic pyroxene, sodic amphibole and phengite compositions from the eclogites in the Çetmi melange. Abbreviations: alm, almandine; adr, andradite; fgl, ferroglaucophane; gln, glaucophane; grs, grossular; mrb, magnesioriebeckite; rbk, riebeckite; sps, spessartine.

estimated from the jadeite content of the sodic pyroxene (Holland, 1990). In terms of its petrology and tectonic setting, the eclogite lens is a typical group C eclogite (Coleman *et al.* 1965).

Phengites from two eclogite samples were dated using the Rb/Sr method. The Rb/Sr data are shown in Table 3. Phengites from both samples gave mid-Cretaceous ages of ~100 Ma. These isotopic ages are compatible with the age of the Çetmi melange.

The rock types, the melange-type internal structure and the presence of eclogites in the Çetmi melange indicate that it represents a Tethyan oceanic accretionary complex. The eclogites must have been injected into the accretionary prism prior to the terminal continental collision. The Triassic and Cretaceous limestone blocks probably represent fragments of a passive continental margin, which was accreted during the initial stages of collision. The youngest limestone blocks in the Çetmi accretionary melange west of Kazdağ are of Turonian–Santonian age. Limestone blocks in the melanges northeast of Gelibolu (Fig. 3) range up to mid-Palaeocene (Montian) in age (Okay & Tansel, 1994), indicating that subduction–accretion continued up to this period. An upper limit on the subduction–accretion and emplacement of the Çetmi accretionary melange is provided by the little deformed Middle Eocene–Oligocene limestones and clastic rocks, which lie unconformably over older sequences in northwest Turkey (Fig. 3). The structures in the Çetmi melange must have formed during the Late Cretaceous–Palaeocene oceanic subduction–accretion, Early Eocene continental collision and latest Oligocene–Early Miocene extension. No attempt has been made to analyse and differentiate these structures.

6. Evciler Pluton: pinning of the shear zone

The Evciler granitoid is an elliptical, calc-alkaline pluton situated north of the Kazdağ range (Fig. 3). It extends northeast–southwest parallel to the trend of the Kazdağ dome and the Alakeçi shear zone. Its mineralogical composition ranges from monzodiorite

through quartz–diorite to granodiorite; the latter is the predominant facies constituting over 70% of the pluton (Öngen, 1978, 1994; Genç, 1998). The Evciler pluton has intruded the Kazdağ Massif, the Alakeçi shear zone and the Çetmi accretionary melange and has folded their contacts (Figs 4, 5). In the north it has intruded into the Late Oligocene–Middle Miocene andesites, dacites and intercalated lacustrine sedimentary rocks (Fig. 3). These volcanic rocks are geochemically close to the Evciler pluton and are regarded as its extrusive equivalents (Genç, 1998).

The Evciler pluton is medium-grained, equigranular and generally undeformed. Pegmatite and aplite veins are frequently observed cross-cutting the foliation in the metamorphic rocks surrounding the pluton. However, near the southern margin of the pluton, there are high temperature shear zones, several metres thick, where the granitoid is foliated and lineated. The foliation and lineation in the granitoid are subparallel to the regional fabric in the adjacent gneisses (Fig. 5), indicating that the Evciler pluton has been partially effected by the extensional deformation. Along this southern contact the foliation in the metamorphic rocks dips north at ~45° under the granitoid, implying that this is the basal contact of the pluton. Metamorphic rocks along this basal contact do not show any contact metamorphism even as near as one metre to the granitoid, indicating that they were at elevated temperatures during the intrusion of the granitoid. In contrast, the limestones in the Çetmi melange are contact metamorphosed into marbles along the northwestern granitoid contact. These observations and the presence of the extrusive equivalents of the granitoid in the north suggest that the Evciler pluton is tilted northwest at ~45°. The pressure of emplacement of the Evciler granitoid, estimated by the Al-in-hornblende geobarometer of Hollister *et al.* (1987) and Schmidt (1992), is 2.6 ± 1 kbar (S. Öngen, unpub. Ph.D. thesis, Univ. Nancy, 1992; T. Ghassap, unpub. Diploma thesis, Univ. Tübingen, 1994) corresponding to a depth of emplacement of ~7 km.

Although there are rare and narrow shear zones within the Evciler pluton, most of the pluton is undeformed and cross-cuts the foliation and lineation in the Kazdağ Massif. It thereby provides an upper age constraint for the ductile exhumation of the metamorphic rocks along the Alakeçi shear zone. Two samples from the Evciler granodiorite were dated using the Rb/Sr method. Sample 5112 is a clinopyroxene- and biotite-bearing diorite collected close to the contact with the Alakeçi shear zone (Fig. 5). Sample 5152 collected eight kilometres east of this contact is a biotite- and hornblende-bearing granodiorite. Both samples gave biotite cooling ages of ~21 Ma (Table 3), essentially identical to the 18–20 Ma biotite Rb/Sr ages from the Kazdağ Massif. Assuming a fast cooling rate, as inferred in the metamorphic rocks, and considering the intrusive nature of the Evciler pluton, the age of intrusion is most likely ~24 Ma, indistinguishable from the age of the high temperature metamorphism. Birkle & Satır (1995) also report a 25 ± 0.3 Ma biotite Rb/Sr age from the Evciler granitoid. This age comes from a sample from the northeastern part of the Evciler pluton and may represent a different sub-intrusion. The isotopic and geobarometric data indicate that the Evciler granodiorite intruded the metamorphic rocks of the Kazdağ Massif during the latest Oligocene at a depth of ~7 km, shortly after the peak deformation and metamorphism. The Evciler pluton is similar to the 17 Ma old late kinematic granodiorite in Tinos in the Cyclades, which also intrudes the lower and upper plates as well as the detachment fault (Avigad & Garfunkel, 1991; Jolivet & Patriat, 1999).

7. Neogene sedimentary and volcanic rocks

Terrigeneous red, coarse clastic rocks up to 200 m thick, with abundant volcanic clasts, lie unconformably over the Çetmi accretionary melange. These pass up into Neogene andesitic lavas and tuffs, over several hundred metres in thickness. The volcanic rocks are overlain unconformably by a sequence of shale, siltstone and tuff, 600 m thick, interpreted as a lacustrine turbidite sequence (Siyako, Bürkan & Okay, 1989). Spores from the shales give an Early to Mid-Miocene age to the lacustrine series (İnci, 1984). Small coal-bearing terrigeneous basins, associated with volcanic rocks, also occur north of Kazdağ. Palynomorph assemblages from coal horizons in the Çan Neogene basin north of Kazdağ give an age range of Late Burdigalian–Early Serravallian (20–15 Ma: Ediger, 1990). The Miocene volcanic and sedimentary rocks are unconformably overlain by fluviatile coarse clastics, which fill the Bayramiç basin northwest of Kazdağ. Similar clastic rocks, 1250 m in thickness, have been encountered in the Edremit-1 petroleum well in the Edremit bay (Siyako, Bürkan & Okay, 1989) (Fig. 3). Their age is regarded as Pliocene–Quaternary.

7.a. Origin of Neogene magmatism in northwest Turkey

Neogene calc-alkaline volcanic rocks are widespread in northwest Turkey (Fig. 3). They range from andesite, trachyandesite to dacite and occur as lava flows, lahars and ignimbrites, as well as widespread tuffs (e.g. Yılmaz, 1990; Seyitoğlu & Scott, 1992; Karacık & Yılmaz, 1998). The K/Ar ages of the volcanic rocks from around the Kazdağ Massif range from 23 Ma to 17 Ma (Fig. 3) and are coeval with the Evciler pluton and with the regional metamorphism in the Kazdağ Massif. The K/Ar and Rb/Sr ages of several granitoidic calc-alkaline plutons in northwest Turkey are also tightly clustered between 25 and 20 Ma.

The geochemistry of the Early Miocene magmatic rocks in the northern Aegean are similar to the

arc-type magmas, and many workers have related their formation to the subduction of the oceanic lithosphere (e.g. Borsi *et al*. 1972; Fytikas *et al.* 1976; Pe-Piper & Piper, 1989). This view is supported by tomographic profiles, which show the presence of an aseismic subducting slab in the northern Aegean at a depth of up to 800 km (Spakman, Wortel & Vlaar, 1988). The length of the subducted slab indicates a minimum age of 26 Ma for the initiation of subduction (Spakman, Wortel & Vlaar, 1988; Meulenkamp *et al.* 1988). This is earlier than ~13 Ma suggested by Le Pichon & Angelier (1979), but fits well with the age and arc-type geochemistry of the magmatic rocks in the northern Aegean. Two objections to this interpretation have been the large distance between the present Hellenic subduction zone and the Early Miocene magmatic rocks in northwest Turkey, and the circular outcrop of the magmatic rocks (Genç, 1998) (Fig. 1). In modern subduction zones the distance between the trench axis and the magmatic arc is 150–200 km (e.g. Windley, 1986, p. 251) much less than the 600 km distance between the Hellenic trench and the Biga peninsula. However, the average amount of extension β across this distance has been 1.5 in the last 13 Ma (Le Pichon & Angelier, 1981), and probably considerably greater since 25 Ma, so that the present day 600 km distance does not represent the arc–trench gap during Early Miocene times.

Modern magmatic arcs form linear belts 50–100 km wide (Windley, 1986, p. 255), quite different than the 250 km by 250 km circular outcrop pattern of the northwest Turkish calc-alkaline province (Fig. 1). However, recent isotopic dating has shown that the volcanic rocks in the northern Biga peninsula and on the island of İmroz (Fig. 3) are Oligocene (37 to 28 Ma) rather than Early Miocene in age (Ercan *et al.* 1996), similar to those in the northeastern Greece (35 to 29 Ma: Eleftheriadis & Lippolt, 1984). The southward younging of magmatic rocks can be explained by the roll-back of the subduction zone during the late Oligocene and Early Miocene. In this view, the Kazdağ as well as the Rhodope crystalline complex were located in the core of an Andean-type magmatic arc during the Early Miocene. The magmatic arc setting of the Kazdağ Massif provides an explanation for the Miocene regional metamorphism of Carboniferous high-grade metamorphic rocks. The complete recrystallization of dry metamorphic rocks requires large influx of fluids, which could have been derived from the subducting slab during the latest Oligocene–Early Miocene.

8. Exhumation of the Kazdağ Massif

The Kazdağ Massif underwent high temperature regional metamorphism during the latest Oligocene (~24 Ma) at a depth of ~14 km. Extensional deformation was synchronous with the regional metamorphism and resulted in the exhumation of the metamorphic rocks from ~14 km to ~7 km along a northward-dipping ductile shear zone. The activity along the shear zone was terminated by the intrusion of a latest Oligocene granitoidic pluton, whose age is analytically indistinguishable from that of the high temperature metamorphism. These temporal and spatial relations indicate very rapid exhumation rates, ~7 mm/yr, which are corroborated by the closely spaced Rb/Sr muscovite and biotite ages. The apparent lack of low-pressure andalusite-bearing mineral assemblages in the Kazdağ metamorphic rocks implies that the rate of exhumation was faster than the rate of equilibration in the rocks. The intrusion of the granitoid terminated the activity of the shear zone, possibly by introducing new volume to the system and thereby absorbing extension (e.g. Parsons & Thompson, 1991). The subsequent exhumation of the Kazdağ Massif to the surface must have occurred along different faults and possibly by a different mechanism.

The Lower–Middle Miocene clastic rocks immediately south and north of Kazdağ are fine-grained lacustrine turbidites with no detritus derived from the Kazdağ Massif. During this period the Kazdağ range must have been a low-lying area, possibly covered by a large lake. Gneiss clasts are first encountered in the fluviatile Pliocene–Quaternary conglomerates and sandstones of the Bayramiç area (Siyako, Bürkan & Okay, 1989). These data suggest that the exhumation of the Kazdağ Massif was a discontinuous, two-stage process. Exhumation in the ductile part of the crust occurred in latest Oligocene times, and in the brittle crust during the Pliocene and Quaternary. The latter period corresponds the activity of the North Anatolian Fault, a major transform fault constituting the boundary between the Eurasian and Anatolian plates (e.g. Şengör, 1979). A major branch of the North Anatolian Fault strikes through the centre of the Biga Peninsula (Barka & Kadinsky-Cade, 1988; Siyako, Bürkan & Okay, 1989). This Biga fault zone consists of NE-trending anastomosing dextral strike-slip segments (Fig. 2). The fault segment between Gönen and Yenice was ruptured during a major earthquake (M_S 7.2) on 18 January 1953 with up to 4 m of dextral displacement (Ketin & Roesli, 1953). The Kazdağ range is situated between two overstepping active fault segments (Fig. 2). Dextral strike-slip along these faults is producing compression and uplift in the area in between. The Güre fault in the south forms the contact between the Kazdağ Massif and an east–west elongated granitoid (Figs 2, 3). Off-shore faults subparallel to the Güre fault control the northern rectilinear margin of the Edremit Bay. Apart from the morphology, the presence of these off-shore faults is inferred from the results of the Edremit-1 petroleum well (Fig. 3). The well, drilled in the eastern part of the bay, has cut through 1250 m thick coarse Quaternary to Pliocene clastic rocks overlying Miocene tuffs and

volcanic rocks, over 1350 m in thickness (Siyako, Bürkan & Okay, 1989). The well data coupled with the present high topography of the Kazdağ range indicate a minimum 4.3 km post-Miocene vertical offset along the faults south of Kazdağ. The present anomalously high topography of the Kazdağ range, as well as its Late Pliocene to Quaternary exhumation, are related to its tectonic setting as a transpressive ridge in a restraining step-over. An implication of this model is that the region of the latest Oligocene metamorphism is larger than suggested by its present outcrop; latest Oligocene metamorphic rocks probably underlie most of the region of the Oligo-Miocene magmatism in northwest Turkey.

9. Discussion and conclusions

The Kazdağ range in northwestern Turkey is an extensional metamorphic core complex of latest Oligocene age. Rocks in the footwall of the core complex consist of gneiss, marble and amphibolite metamorphosed during the latest Oligocene at 640 ± 50 °C and 5 ± 1 kbar. The hangingwall is made up of an Early Tertiary accretionary melange with exotic Upper Cretaceous eclogite blocks. The two are separated by a ductile shear zone of ultramylonite, two kilometres thick (Fig. 4). Both the high-grade metamorphic rocks and the mylonites show a N-trending lineation with a top-to-the north shear sense.

The Aegean region is known to have undergone significant but locally variable rotations since the Early Miocene (e.g. Kissel & Laj, 1988). Nevertheless, palaeomagnetic data from the Lower Miocene calc-alkaline lava flows in the Biga peninsula and in Lesbos show no significant rotations (Kissel *et al.* 1987). Hence, the N-trending lineations in the Kazdağ can be accepted as representing the direction of the latest Oligocene–Early Miocene extension. This direction is at variance with the model of Jolivet *et al.* (1994), who describe the extension in the Aegean region during the last 25 m.y. by rotation along two poles located at either ends of the Hellenic arc. This model predicts NE- (N64°E) trending rather than the observed N- (N12°E) trending stretching lineations in the Biga Peninsula. Furthermore, recent palaeomagnetic data from the Cyclades have indicated that the NE-trending lineations from Evvia to Mykonos (Fig. 1), are a result of post-Late Miocene clockwise rotations (Morris & Anderson, 1996; Avigad, Baer & Heimann, 1998). When reconstructed the original stretching directions in the central Aegean become more northerly similar to those observed in the Kazdağ region.

The exhumation of the Kazdağ Massif was a two-stage process. Exhumation from a depth of ~14 km to ~7 km occurred at ~24 Ma along a ductile shear zone. Activity along the shear zone was terminated by the intrusion of a latest Oligocene (~24 Ma) granitoid. Subsequent exhumation to the surface occurred during the Pliocene–Quaternary (after 5 Ma) along brittle faults of the North Anatolian Fault system. The anomalously high topography of the Kazdağ range is related to its ongoing uplift as a compressive ridge between two overstepping dextral strike-slip faults of the North Anatolian Fault zone.

Gravitational or orogenic collapse, which involves downhill transport from regions of high topography to regions of low topography (Dewey, 1988) has been suggested as a mechanism driving the extension in the Aegean (Berckhemer, 1977; Seyitoğlu & Scott, 1996). The alternate hypothesis is extension by the retreat or rollback of the subducting plate (Dewey, 1980). The former hypothesis requires high topography prior to the inception of extension. The widespread blueschists and eclogites in the central Aegean have been cited as evidence for a thick, and consequently topographically high, continental crust prior to the onset of extension. However, in northwest Turkey there is no evidence for a high topography during the Eocene and Oligocene. Rocks of this age are preserved in the northern Biga and Gelibolu peninsulas as well as in the Thrace basin (Figs 1, 3) and are predominantly marine. The flora in the Early Miocene continental sediments in northwest Turkey indicates a sub-tropical climate (e.g. Mädler & Steffens, 1979; Ediger, 1990) unlikely for high altitutes. Ironically, in the Biga Peninsula, eclogites occur in the hangingwall rather than in the footwall of the core complex, and their Late Cretaceous ages indicate that they were exhumed prior to the latest Oligocene extension. In northwest Turkey the continental crust is at present ~35 km thick (Makris, 1977; Le Pichon & Angelier, 1981). It could be argued that metamorphic rocks in the Kazdağ range, formed at a depth of ~14 km during the latest Oligocene, imply a Late Oligocene crustal thickness of ~50 km. However, during the Early Miocene there was a net magmatic addition to the continental crust of northwest Turkey in terms of voluminous calc-alkaline volcanic and plutonic rocks. The Nd and Sr initial ratios of these magmatic rocks indicate a major mantle-derived component (Birkle & Satır, 1995). Hence, the crustal thickness before the onset of extension in northwest Turkey was most probably not too different from the present, as suggested by the stratigraphic and paleontological data. This implies that gravitational collapse has not been the main driving mechanism for extension in the Kazdağ core complex.

In northwest Turkey the age of the voluminous calc-alkaline volcanic and plutonic rocks overlaps with the latest Oligocene high-temperature metamorphism (Fig. 11), implying that mantle-driven magmatism rather than relaxing geotherms in a thickened crust are the heat source of the metamorphism. Geochemical and seismic tomographic data indicate that these magmatic rocks form part of a Late Oligocene–Early Miocene magmatic arc above the Hellenic subduction zone. The Kazdağ Massif and the Rhodope metamor-

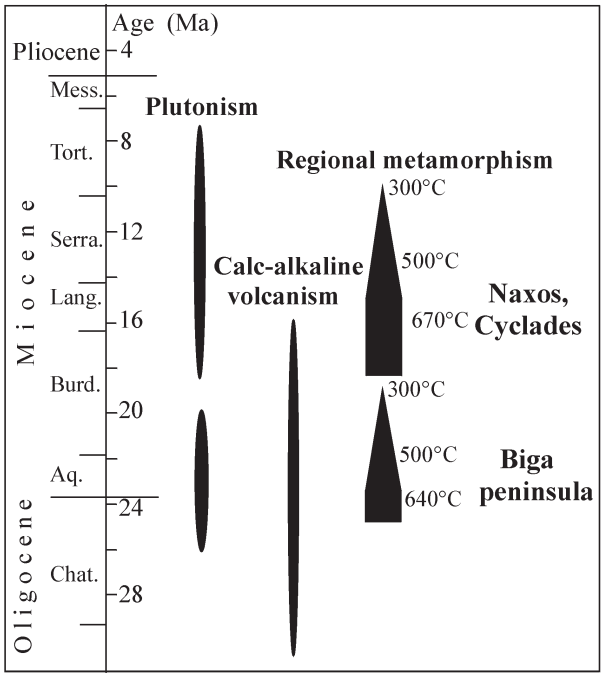

Figure 11. Oligocene–Miocene plutonic, volcanic and metamorphic events in the Biga peninsula and in the Cyclades. The Naxos data is from Altherr *et al.* (1982); Schliestedt, Altherr & Matthews (1987); Wijbrans & McDougall (1988); Buick (1991); Gautier, Brun & Jolivet (1993). Note the southward progression of magmatism and metamorphism possibly following a southward migrating magmatic arc. The apparent absence of volcanism in the Cyclades may be due to subsequent erosion.

phic complex, which exhibit similar magmatic and metamorphic histories (Dinter *et al*. 1995; Wawrzenitz & Krohe, 1998), were located in the core of this magmatic arc. The latest Oligocene extension in northwest Turkey could therefore be initiated by the subduction roll-back of the Hellenic trench. Further support for this view comes from the core complexes in the central Aegean (e.g. Buick, 1991; Lee & Lister, 1992; Gautier, Brun & Jolivet, 1993). The Cycladic core complexes, especially that on Naxos, are similar in many aspects to the Kazdağ core complex. The major difference between the two is in the timing of events (Fig. 11). The high temperature metamorphism, related extensional deformation and late kinematic plutonism are Mid- to Late Miocene (16–10 Ma) in the Naxos (Altherr *et al.* 1982; Schliestedt, Altherr & Matthews, 1987; Wijbrans & McDougall, 1988; Andriessen, 1991) and latest Oligocene–Early Miocene (27–19 Ma) in the Kazdağ and Rhodope core complexes. The southward progression of the extensional deformation and metamorphism in the Aegean are most probably related to the southward migration of the magmatic arc. Jolivet *et al*. (1998) observe a similar pattern of migration of extension and arc magmatism in the Tyrrhenian Sea and compare it with the case in the Aegean, and suggest that both are related to the slab roll-back.

According to the isotopic age data the subduction-related magmatism started in the Biga Peninsula by ~30 Ma (Fig. 3). The heat pulse associated with this magmatism must have thermally softened the crust and localized the extension, as has been inferred in many other core complexes (e.g. Armstrong & Ward, 1991; Lister & Baldwin, 1993). The magmatic arc must have also provided the heat and the fluids necessary for the latest Oligocene metamorphism. A close spatial and temporal link between core-complex formation and magmatic activity exists in many other regions, including in the Basin and Range province (e.g. Gans, Mahood & Schermer, 1989; Armstrong & Ward, 1991), in the Solomon Sea, Papua New Guinea (Baldwin *et al*. 1993) and in the northern Tyrrhenian Sea (Jolivet *et al.* 1998).

Compressional (Yılmaz, 1990) and extensional tectonic settings (Seyitoğlu & Scott, 1992) have been suggested for the Late Oligocene–Early Miocene calc-alkaline magmatism in northwestern Turkey. Data from the Kazdağ Massif indicate unambiguously that the magmatism occurred in a north–south extending crust. The extension might have contributed to the solution of the space problem posed by the Late Oligocene–Early Miocene intrusions in the Biga peninsula (Fig. 3).

Acknowledgements. This study was supported by the Turkish Petroleum Company (TPAO) and by the TÜBİTAK grant YDABÇAG-419/G. We thank Demir Altıner, Leopold Krystyn, the late Murat Köylüoğlu, and İzver Tansel for paleontological determinations, Kerem Ali Bürkan, Thomas Ghassap, Muzaffer Siyako, and Burak Yıkılmaz for help during the field work. Helpful reviews by Dov Avigad and Laurent Jolivet are gratefully acknowledged.

References

Altherr, R., Kreuzer, H., Wendt, I., Lenz, H., Wagner, G. A., Keller, J., Harre, W. & Hoehndorf, A. 1982. A late Oligocene/Early Miocene high temperature belt in the Attic Cycladic Crystalline Complex (Greece). *Geologisches Jahrbuch* **E23**, 97–164.

Andriessen, P. A. M. 1991. K–Ar and Rb–Sr age determinations on micas of impure marbles of Naxos, Greece: The influence of metamorphic fluids and lithology on the blocking temperature. *Schweizerische Mineralogische und Petrographische Mitteilungen* **71**, 89–99.

Anil, M., Saupe, F., Zimmermann, J. L. & Öngen, S. 1989. K/Ar age determination of the Oligo-Miocene Nevruz-Çakıroba (Yenice-Çanakkale) quartz-monzonite stocks. *43rd Geological Congress of Turkey, Abstracts*, pp. 25–6.

Armstrong, R. L. & Ward, P. 1991. Evolving geographic pattern of Cenozoic magmatism in the North American Cordillera: The temporal and spatial association of magmatism and metamorphic core complexes. *Journal of Geophysical Research* **B96**, 13201–24.

Ataman, G. 1974. Revue geochronologie des massifs plutoniques et metamorphiques de l'Anatolie. *Hacettepe Bulletin of Natural Sciences and Engineering* **3**, 75–87.

Ataman, G. 1975. Plutonisme calco-alkalin d'age Alpin en Anatolie du Nordquest. *Comptes Rendus de l'Académie des Sciences, Paris* **D280**, 2065–8.

AVIGAD, D., BAER, G. & HEIMANN, A. 1998. Block rotations and continental extension in the central Aegean Sea: palaeomagnetic and structural evidence from Tinos and Mykonos (Cyclades, Greece). *Earth and Planetary Science Letters* **157**, 23–40.

AVIGAD, D. & GARFUNKEL, Z. 1991. Uplift and exhumation of high-pressure metamorphic terrains: the example of the Cycladic blueschist belt (Aegean Sea). *Tectonophysics* **188**, 357–72.

BALDWIN, S. L., LISTER, G. S., HIIL, E. J., FOSTER, D. A. & MCDOUGALL, I. 1993. Thermochronological constraints on the tectonic evolution of active metamorphic core complexes, D'Entrecasteaux islands, Papua New Guinea. *Tectonics* **12**, 611–28.

BARKA, A. A. & KADINSKY-CADE, K. 1988. Strike-slip fault geometry in Turkey and its influence on earthquake activity. *Tectonics* **7**, 663–84.

BERCKHEMER, H. 1977. Some aspects of the evolution of marginal seas deduced from observations in the Aegean region. In *Structural History of the Mediterranean Basins* (eds B. Biju-Duval and L. Montadert), pp. 303–14. Paris: Technip.

BERGGREN, W. A., KENT, D. V., FLYNN, J. J. & COUVERING, J. A. VAN. 1985. Cenozoic geochronology. *Geological Society of America Bulletin* **96**, 1407–18.

BINGÖL, E. 1969. Geology of the central and southeastern parts of the Kazdağ Massif (in Turkish). *Maden Tetkik ve Arama Enstitüsü Dergisi* **72**, 110–23.

BINGÖL, E., AKYÜREK, B. & KORKMAZER, B. 1975. Geology of the Biga Peninsula and some characteristics of the Karakaya blocky series. In *Proceedings of the Congress of Earth Sciences for the 50th Anniversary of the Republic of Turkey*, pp. 70–7. Ankara, Maden Tetkik ve Arama Enstitüsü.

BINGÖL, E., DELALOYE, M. & ATAMAN, G. 1982. Granitic intrusions in western Anatolia, a contribution to the geodynamic study of this area. *Eclogae Geologicae Helvetiae* **75**, 437–46.

BINGÖL, E., DELALOYE, M., PIŞKIN, Ö. & GENÇ, Ş. 1992. Significance of the granitoids of eastern and southern Marmara within the framework of the regional geotectonic evolution. *Abstracts of the International Symposium on the Geology of the Black Sea Region*, Ankara, p. 3.

BIRKLE, P. & SATIR, M. 1995. Dating, geochemistry and geodynamic significance of the Tertiary magmatism of the Biga-Peninsula (Ezine, NW-Turkey). In *Geology of the Black Sea Region* (eds A. Erler, T. Ercan, E. Bingöl and S. Örçen), pp. 171–80. Ankara: General Directorate of Mineral Research and Exploration.

BORSI, S., FERRARA, G., INNOCENTI, F. & MAZZUOLI, R. 1972. Geochronology and petrology of the recent volcanics in the eastern Aegean sea (West Anatolia and Lesvos Island). *Bulletin of Volcanology* **36**, 473–96.

BOZKURT, E. & PARK, R. G. 1994. Southern Menderes Massif; an incipient metamorphic core complex in western Anatolia, Turkey. *Journal of the Geological Society, London* **151**, 213–16.

BRINKMANN, R. 1976. *Geology of Turkey*. Amsterdam: Elsevier, 158 pp.

BRINKMANN, R., GÜMÜŞ, H., PLUMHOFF, F. & SALAH, A. A. 1977. Höhere Oberkreide in Nordwest-Anatolien und Thrakien. *Neues Jahrbuch für Geologie und Paläontologie, Abhandlungen* **154**, 1–20.

BUICK, I. S. 1991. The late Alpine evolution of an extensional shear zone, Naxos, Greece. *Journal of the Geological Society, London* **148**, 93–103.

CLIFF, R. A. 1985. Isotopic dating in metamorphic belts. *Journal of the Geological Society, London* **142**, 97–110.

COLEMAN, R. G., LEE, D. E., BEATTY, L. B. & BRANNOCK, W. W. 1965. Eclogites and eclogites: Their differences and similarities. *Geological Society of America Bulletin* **76**, 483–508.

COLLINS, A. S. & ROBERTSON, A. H. F. 1998. Processes of Late Cretaceous to Late Miocene episodic thrust-sheet translation in the Lycian Taurides, SW Turkey. *Journal of the Geological Society, London* **155**, 759–72.

DEWEY, J. F. 1980. Episodicity, sequence and style at convergent plate boundaries. In *The Continental Crust and its Mineral Deposits* (ed. D. W. Strangway), pp. 553–73. Geological Association of Canada, Special Paper no. 20.

DEWEY, J. F. 1988. Extensional collapse of orogens. *Tectonics* **7**, 1123–39.

DEWEY, J. F. & ŞENGÖR, A. M. C. 1979. Aegean and surrounding regions: complex multiplate and continuum tectonics in a convergent zone. *Bulletin of the Geological Society of America* **90**, 84–92.

DINTER, D. A., MACFARLANE, A. M., HAMES, W., ISACHSEN, C., BOWRING, S. & ROYDEN, L. 1995. U–Pb and $^{40}Ar/^{39}Ar$ geochronology of the Symvolon granodiorite: Implications for the thermal and structural evolution of the Rhodope metamorphic core complex, northeastern Greece. *Tectonics* **14**, 886–908.

DINTER, D. A. & ROYDEN, L. 1993. Late Cenozoic extension in northeastern Greece: Strymon Valley detachment and Rhodope metamorphic complex. *Geology* **21**, 45–8.

EDIGER, V. Ş. 1990. Paleopalynology of coal-bearing Miocene sedimentary rocks associated with volcanics of the Biga Peninsula (NW Turkey) and the effect of volcanism on vegetation. *Neues Jahrbuch für Geologie und Paläontologie, Abhandlungen* **180**, 259–77.

ELEFTHERIADIS, G. & LIPPOLT, H. J. 1984. Altersbestimmungen zum oligäzenen Vulkanismus der Süd Rhodopen/Nord Griechenland. *Neues Jahrbuch für Geologie, Paläontologie, Monatshefte* **3**, 179–91.

ELLIS, D. J. & GREEN, D. H. 1979. An experimental study of the effect of Ca upon garnet-clinopyroxene Fe–Mg exchage equilibria. *Contributions to Mineralogy and Petrology* **71**, 12–22.

ERCAN, T., SATIR, M., STEINITZ, G., DORA, A., SARIFAKIOĞLU, E., ADIS, C., WALTER, H-J. & YILDIRIM, T. 1996. Features of the Tertiary volcanism in the Biga Peninsula and in the islands of Gökçeada, Bozcaada and Tavşan adası (in Turkish). *Maden Tetkik ve Arama Dergisi* **117**, 55–86.

EVANS, B. W. 1977. Metamorphism of Alpine peridotite and serpentinite. *Annual Reviews of the Earth and Planetary Sciences* **5**, 397–447.

FYTIKAS, M., GIULIANI, O, INNOCENTI, F., MARINELLI, G. & MAZZUOLI, R. 1976. Geochronological data on recent magmatism of the Aegean Sea. *Tectonophysics* **31**, 29–34.

GANS, P. B., MAHOOD, G.A. & SCHERMER, E. R. 1989. *Synextensional magmatism in the Basin and Range province; a case study from the eastern Great basin.* Geological Society of America, Special Paper no. 233, 60 pp.

GAUTIER, P., BRUN, J.-P. & JOLIVET, L. 1993. Structure and kinematics of Upper Cenozoic extensional detachment on Naxos and Paros (Cyclades islands, Greece). *Tectonics* **12**, 1180–94.

GENÇ, Ş.C. 1998. Evolution of the Bayramiç magmatic complex, northwestern Anatolia. *Journal of Volcanology and Geothermal Research* **85**, 233–49.

Gutnic, M., Monod, O., Poisson, A. & Dumont, J. F. 1979. Géologie des Taurides Occidentales (Turquie). *Mémoires de la Sociéte Géologique de France* **137**, 1–112.

Hetzel, R., Ring, U., Akal, C. & Troesch, M. 1995. Miocene NNE-directed extensional unroofing in the Menderes Massif, southwestern Turkey. *Journal of the Geological Society, London* **152**, 639–54.

Hodges, K. V. & Spear, F. S. 1982. Geothermometry, geobarometry and the Al_2SiO_5 triple point at Mt. Moosilauke, New Hampshire. *American Mineralogist* **67**, 118–34.

Holland, T. J. B. 1990. Activities of components in omphacitic solid solutions. *Contributions to Mineralogy and Petrology* **105**, 446–53.

Holland, T. J. B. & Powell, R. 1990. An enlarged and updated internally consistent thermodynamic data set with uncertainties and correlations: the system K_2O–Na_2O–CaO–MgO–MnO–FeO–Fe_2O_3–Al_2O_3–TiO_2–SiO_2–C–H_2O–O_2. *Journal of Metamorphic Geology* **8**, 89–124.

Hollister, L. S., Grissom, G. C., Peters, E. K., Stowell, H. H. & Sisson, V. B. 1987. Confirmation of the empirical correlation of Al in hornblende with pressure of solidification of calcalkaline plutons. *American Mineralogist* **72**, 231–9.

Inci, U. 1984. Stratigraphy and organic features of the bituminous shales from Demirci and Burhaniye (in Turkish). *Türkiye Jeoloji Kurumu Bülteni* **5**, 27–40.

Jäger, E., Niggli, E. & Wenk, E. 1967. Rb–Sr Altersbestimmungen an Glimmern der Zentralalpen. *Beiträge zu der geologische Karte der Schweiz* **NF134**, 67 pp.

Jolivet, L., Brun, J.-P., Gautier, P., Lallemant, S. & Patriat, M. 1994. 3D-kinematics of extension in the Aegean region from the early Miocene to the Present, insights from the ductile crust. *Bulletin de la Société Géologique de France* **165**, 195–209.

Jolivet, L., Faccenna, C., Goffe, B., Mattei, M., Rossetti, F., Brunet, C., Storti, F., Funiciello, R., Cadet, J. P., d'Agostina, N. & Parra, T. 1998. Midcrustal shear zones in postorogenic extension: Example from the northern Tyrrhenian Sea. *Journal of Geophysical Research* **103**, 12123–60.

Jolivet, L. & Patriat, M. 1999. Ductile extension and the formation of the Aegean Sea. In *The Mediterranean basins: Tertiary Extension within the Alpine Orogen* (eds B. Durand, L. Jolivet, F. Horvath and M. Seranne), pp. 427–56. Geological Society of London, Special Publication no. 156.

Karacik, Z. & Yilmaz, Y. 1998. Geology of the ignimbrites and the associated volcano-plutonic complex of the Ezine area, northwest Anatolia. *Journal of Volcanology and Geothermal Research* **85**, 251–64.

Ketin, İ. & Roesli, F. 1953. Makroseismische Untersuchungen über das nordwestanatolischen Beben vom 18. März 1953. *Eclogae Geologicae Helvetiae* **46**, 187–208.

Kissel, C. & Laj, C. 1988. The Tertiary geodynamical evolution of the Aegean arc: a paleomagnetic reconstruction. *Tectonophysics* **146**, 183–201.

Kissel, C., Laj, C., Şengör, A. M. C. & Poisson, A. 1987. Paleomagnetic evidence for rotation in opposite senses of adjacent blocks in northeastern Aegea and western Anatolia. *Geophysical Research Letters* **14**, 907–10.

Koziol, A. M. & Newton, R. C. 1988. Redetermination of the anorthite breakdown reaction and improvement of the plagioclase–garnet–Al_2SiO_5–quartz geobarometer. *American Mineralogist* **73**, 216–33.

Krushensky, R. D. 1976. Neogene calc-alkaline extrusive and intrusive rocks of the Karalar-Yeşiller area, northwest Anatolia. *Bulletin of Volcanology* **40**, 336–60.

Lee, J. & Lister, G. S. 1992. Late Miocene ductile extension and detachment faulting, Mykonos, Greece. *Geology* **20**, 121–4.

Le Pichon, X. & Angelier, J. 1979. The Hellenic arc and trench system: A key to the neotectonic evolution of the Eastern Mediterranean area. *Tectonophysics* **60**, 1–42.

Le Pichon, X. & Angelier, J. 1981. The Aegean Sea. *Philosophical Transactions of the Royal Society, London* **A 300**, 357–72.

Leven, E. J. & Okay, A.I. 1996. Foraminifera from the exotic Permo-Carboniferous limestone blocks in the Karakaya Complex, northwest Turkey. *Rivista Italiana Paleontologia e Stratigrafia* **102**, 139–74.

Lister, G. S. & Baldwin, S. L. 1993. Plutonism and the origin of metamorphic core complexes. *Geology* **21**, 607–10.

Lister, G. S., Banga, G. & Feenstra, A. 1984. Metamorphic core complexes of Cordilleran type in the Cyclades, Aegean Sea, Greece. *Geology* **12**, 221–5.

Mädler, K. & Steffens, P. 1979. Neue Blätterfloren aus dem Oligozän, Neogen und Pleistozän der Türkei. *Geologisches Jahrbuch* **33**, 3–33.

Makris, J. 1977. Geophysical investigations in the Hellenides. *Hamburger Geophysikalische Einzelschriften* **34**, 124 pp.

McKenzie, D. P. 1972. Active tectonics of the Mediterranean region. *Geophysical Journal of the Royal Astronomical Society* **30**, 109–85.

Meulenkamp, J. E., Wortel, M. J. R., van Wamel, W. A., Spakman, W. & Strating, E. H. 1988. On the Hellenic subduction zone and the geodynamic evolution of Crete since the late Middle Miocene. *Tectonophysics* **146**, 203–15.

Morris, A. & Anderson, M. 1996. First palaeomagnetic results from the Cycladic Massif, Greece, and their implications for Miocene extension directions and tectonic models in the Aegean. *Earth and Planetary Science Letters* **142**, 397–408.

Newton, R. C. & Perkins, D. III. 1982. Thermodynamic calibration of geobarometers based on the assemblages garnet–plagioclase–orthopyroxene (clinopyroxene)–quartz. *American Mineralogist* **67**, 203–22.

Okay, A. I., Satir, M., Maluski, H., Siyako, M., Monie, P., Metzger, R. & Akyüz, S. 1996. Paleo- and Neo-Tethyan events in northwest Turkey: geological and geochronological constraints. In *Tectonics of Asia* (eds A. Yin and M. Harrison), pp. 420–41. Cambridge University Press.

Okay, A. I., Şengör, A. M. C. & Satir, M. 1993. Tectonics of an ultra-high pressure metamorphic terrane: the Dabie Shan/Tongbai Shan orogen, China. *Tectonics* **12**, 1320–34.

Okay, A. I., Siyako, M. & Bürkan, K. A. 1991. Geology and tectonic evolution of the Biga peninsula, northwest Turkey. *Bulletin Technical University of Istanbul* **44**, 191–256.

Okay, A. I. & Tansel, İ. 1994. New data on the upper age of the Intra-Pontide ocean from north of Şarköy (Thrace). *Bulletin of the Mineral Research and Exploration* **114**, 23–6.

Okrusch, M. & Bröcker, M. 1990. Eclogites associated with high-grade blueschists in the Cyclades archipelago, Greece: A review. *European Journal of Mineralogy* **2**, 451–78.

Öngen, S. 1978. Petrographie und Petrochemie des Çavuşlu-Karaköy Granitoid Massivs, *İstanbul Üniversitesi Fen Fakültesi Mecmuası* **B43**, 93–115.

Öngen, S. 1994. Le pluton calco-alcalin d'Evciler (peninsula de Biga, Turquie-NW): age, geochemie et signification geodynamique. *Comptes Rendus de l'Académie des Sciences, Paris* **319**, 1033–9.

Papanikolaou, D. J. & Demirtaşli, E. 1987. Geological correlations between the Alpine segments of the Hellenides-Balkanides and Taurides-Pontides. In *Pre-Variscan and Variscan Events in the Alpine-Mediterranean Mountain Belts* (eds H. W. Flügel, F. P. Sassi and P. Grecula), pp. 387–96. Bratislava: Alfa Publishers.

Parsons, T. & Thompson, G. A. 1991. The role of magma overpressure in suppressing earthquakes and topography: World-wide examples. *Science* **253**, 1399–1402.

Pe-piper, G. 1980. Geochemistry of Miocene shoshonites, Lesbos, Greece. *Contributions to Mineralogy and Petrology* **72**, 387–96.

Pe-piper, G. & Piper, D. J. W. 1989. Spatial and temporal variation in late Cenozoic back-arc volcanic rocks, Aegean Sea region. *Tectonophysics* **169**, 113–34.

Pickett, E. A. & Robertson, A. H. F. 1996. Formation of the Late Paleozoic–Early Mesozoic Karakaya Complex and related ophiolites in NW Turkey by Paleotethyan subduction-accretion. *Journal of the Geological Society, London* **153**, 995–1009.

Schliestedt, M., Altherr, R. & Matthews, A. 1987. Evolution of the Cycladic crystalline complex: petrology, isotope geochemistry and geochronology. In *Chemical Transport in Metasomatic Processes* (ed. H. C. Helgeson), pp. 389–428. Reidel Publishing Company.

Schmidt, M. W. 1992. Amphibole composition in tonalite as a function of pressure. an experimental calibration of the Al-in-hornblende-geothermometer. *Contributions to Mineralogy and Petrology* **110**, 304–10.

Schuiling, R. D. 1959. Über eine prä-herzynische Faltungsphase im Kazdağ Kristallin. *Bulletin of the Mineral and Research Exploration Institute, Turkey* **53**, 89–93.

Şengör, A. M. C. 1979. The North Anatolian transform fault: its age, offset and tectonic significance. *Journal of the Geological Society*, *London* **136**, 269–82.

Şengör, A. M. C., Satir, M. & Akkök, R. 1984. Timing of tectonic events in the Menderes massif, western Turkey: implications for tectonic evolution and evidence for Pan-African basement in Turkey. *Tectonics* **3**, 693–707.

Seyitoğlu, G. & Scott, B. C. 1992. Late Cenozoic volcanic evolution of the northeastern Aegean region. *Journal of Volcanology and Geothermal Research* **54**, 157–76.

Seyitoğlu, G. & Scott, B. C. 1996. The cause of N–S extensional tectonics in western Turkey: Tectonic escape vs back-arc spreading vs orogenic collapse. *Journal of Geodynamics* **22**, 145–53.

Seyitoğlu, G., Scott, B. C. & Rundle, C. C. 1992. Timing of Cenozoic extensional tectonics in west Turkey. *Journal of the Geological Society, London* **149**, 533–8.

Siyako, M., Bürkan, K. A. & Okay, A. I. 1989. Tertiary geology and hydrocarbon potential of the Biga and Gelibolu peninsulas (in Turkish). *Türkiye Petrol Jeologları Derneği Bülteni* **1**, 183–200.

Sokoutis, D., Brun, J. P., van de Driessche, J. & Pavlides, S. 1993. A major Oligocene–Miocene detachment in southern Rhodope controlling north Aegean extension. *Journal of the Geological Society, London* **150**, 243–6.

Spakman, W., Wortel, M. J. R. & Vlaar, N. J. 1988. The Hellenic subduction zone: a tomographic image and its geodynamic implications. *Geophysical Research Letters* **15**, 60–3.

Straub, C. & Kahle, H. G. 1995. Active crustal deformation in the Marmara Sea region, NW Anatolia, inferred from GPS measurements. *Geophysical Research Letters* **22**, 2533–6.

Sulzer, H. 1990. Tektonik und Gefügeentwicklung im Kristallin südlichen Biga-Halbinsel (Westanatolien). *Berliner Geowissenschaftliche Abhandlungen* **A127**, Berlin, 74 pp.

Villa, I. M. 1997. Isotopic closure. *Terra Nova* **10**, 42–7.

Walcott, C. R. & White, S. H. 1998. Constraints on the kinematics of postorogenic extension imposed by stretching lineations in the Aegean region. *Tectonophysics* **298**, 155–75.

Wawrzenitz, N. & Krohe, A. 1998. Exhumation and doming of the Thasos metamorphic core complex (S Rhodope, Greece); Structural and geochronological constraints. *Tectonophysics* **285**, 301–32.

Wijbrans, J. R. & McDougall, I. 1988. Metamorphic evolution of the Attic Cycladic metamorphic belt on Naxos (Cyclades, Greece) utilising $^{40}Ar/^{39}Ar$ age spectrum measurements. *Journal of Metamorphic Geology* **6**, 571–94.

Windley, B. F. 1986. *The Evolving Continents*. Second edition, John Wiley & Sons Ltd., 399 pp.

Yilmaz, Y. 1990. Comparison of young volcanic associations of western and eastern Anatolia formed under a compressional regime: a review. *Journal of Volcanology and Geothermal Research* **44**, 69–87.